J. Fluid Mech. (1994), vol. 266, pp. 33–68

Asymptotic analysis of the radiation by volume sources in supersonic rotor acoustics

By H. ARDAVAN
Institute of Astronomy, University of Cambridge, Madingley Road, Cambridge CB3 0HA, UK

(Received 8 April 1991 and in revised form 9 September 1993)

The application of Lighthill's acoustic analogy to the generation of sound by rotating surfaces with supersonic speeds results in radiation integrals in which the stationary points of the phase function – that describes the space-time distance between each source point and a fixed observation point – have variable positions and coalesce at a caustic in the space of source points. Here, the leading term in the asymptotic expansion of the corresponding Green's function at this caustic is calculated, both in the time and the frequency domains, and it is shown that the radiation generated by volume sources, which are steady in the uniformly rotating blade-fixed frame, has an amplitude that does not obey the spherical spreading law, i.e. does not fall off like R_P^{-1} with the radial distance R_P away from the source. Within a finite solid angle, depending on the extent of the source distribution, the amplitude of this newly identified sound decays like $R_P^{-\frac{1}{2}}$, so that it is stronger in the far field than any previously studied element. That this is not incompatible with the conservation of energy is because the emission time intervals associated with the volume elements of the source distribution which contribute towards the non-spherically decaying component of the radiation are by a large (R_P-dependent) factor greater than the time intervals during which the signals generated by these elements are received. The contributing source elements are those whose positions at the retarded time coincide with the locus of singularities of the Green's function, i.e. with the one-dimensional locus of points, fixed in the rotating frame, which approach the observer with the wave speed and zero acceleration along the radiation direction. Because the signals received at two neighbouring instants in time arise from distinct, coherently radiating filamentary parts of the source which have both different extents and different strengths, the resulting overall waveform in the far zone consists of the superposition of a (continuous) set of narrow subpulses with uneven amplitudes. These subpulses are narrower the larger the distance from the source.

The differences between the new results and those of the earlier works in the literature are shown to arise from the error terms in the far-field and high-frequency approximations, approximations that are inappropriate for volume sources moving supersonically.

1. Introduction

It is known, in the context of the sonic boom, that the amplitude of the acoustic radiation generated by a rectilinearly moving supersonic source falls off with the radial distance R_P from the source like $R_P^{-\frac{1}{2}}$, rather than R_P^{-1}, on the Mach cones which issue from the constituent volume elements of the source (Whitham 1974, p. 227; Dowling & Ffowcs Williams 1983, p. 196; see also Appendix A). This notwithstanding, the existing analyses in the literature of the acoustic radiation from *rotating* supersonic sources are based, almost without exception, on the standard far-field approximation to the retarded solution of the wave equation according to which the sound decays spherically, i.e. like R_P^{-1} (see e.g. Hawkings & Lowson 1974; Hanson & Fink 1979; Farassat 1981; Tam, Salikuddin & Hanson, 1988; Crighton & Parry 1991; Peake & Crighton 1991*a*, *b*; the only exceptions known to the author are the works of Ffowcs Williams & Hawkings 1969; and Myers & Farassat 1987). We shall see in this paper that in the case of a (hovering) rotor with a supersonic tip speed, too, the radiation that arises from volume-distributed sources decays cylindrically in the linear regime†: it falls off like $R_P^{-\frac{1}{2}}$ within a wide range of colatitudes, satisfying cosec $\theta_P < r_0\,\omega/c$, on both sides of the plane of rotation ($\theta_P = \frac{1}{2}\pi$), where r_0 and ω are respectively the radius and the (constant) angular velocity of the rotor, and c is the speed of sound in the undisturbed medium.

This decay rate can in fact be established without a knowledge of the values of the various source terms in the Ffowcs Williams–Hawkings equation; the only feature of the source distribution that dictates this, as well as the other results of the present paper, is that it is steady in the blade-fixed rotating frame, i.e. that the flow variables that enter the expression for its density s are functions of the azimuthal angle φ and the time t in the combination $\varphi - \omega t \equiv \hat{\varphi}$ only. The assumption central to an important part of rotor acoustics, that the flow in the blade-fixed frame is steady, implies that the source distribution has a rigidly rotating pattern from the point of view of an observer in the inertial frame, irrespective of what the dependence of s on the cylindrical coordinates $(r, \hat{\varphi}, z)$ of the blade-fixed frame may be. Even though the fluid motion around the rotor, which creates the source with the density s, has velocities that are much smaller than that of sound when the rotor blade is thin, the phase velocity of the pattern associated with the source distribution exceeds c beyond the sonic cylinder $r = c/\omega$. It is the supersonic propagation, around the rotation axis, of this pattern that determines the Green's function for the relevant version of the Ffowcs Williams–Hawking's equation and so underlies the explanation for a host of phenomena in rotor acoustics (see Ardavan 1991*a*, *b*).

The convolution of the Green's function in question, the spiral Green's function – which is simply the sound generated by a source point in circular motion – with the density $s(r, \hat{\varphi}, z)$ of the source distribution in the blade-fixed frame results in a sound amplitude that is the same as what one would obtain by superposing the contributions from the circularly moving volume elements of a source in rigid rotation (see §2). We shall from now on refer to the volume elements of this rigidly rotating source distribution simply as 'source elements' or 'source points'.

Just as the spherical field wavelets emanating from a rectilinearly moving supersonic point source would form a Mach cone at which the field is infinite, so the envelope of the corresponding wavelets from a circularly moving supersonic point source constitutes a caustic at which the spiral Green's function diverges. (These amplitudes are infinitely large for a source that is point-like, but they are finite for an infinitesimal volume element of an extended source.) This caustic begins issuing from the point source in the form of a cone with the same opening angle as that of a Mach cone and, after joining a second sheet, eventually develops into a tube-like surface which spirals around the rotation axis (see figure 1). The two sheets of the caustic are tangent to one another and so form a cusp where they meet. The resulting cusp is a distorted U-shaped

† We shall be concerned only with the linear theory in this paper; it will, in due course, be possible to incorporate the modifications that arise from nonlinear effects with the use of the techniques developed by Whitham (1974) and Lighthill (1993).

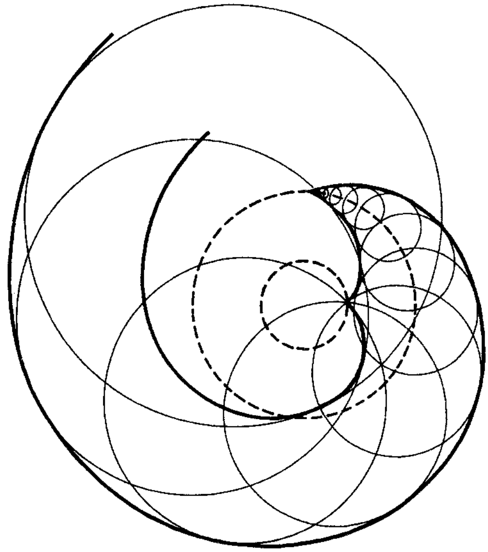

FIGURE 1. The envelope of the spherical field wavelets emanating from a supersonically moving source point in circular motion. The heavier curves show the cross-section of the envelope with the plane of the orbit of the source. The larger of the two broken circles designates the orbit and the smaller the sonic cylinder $r = c/\omega$.

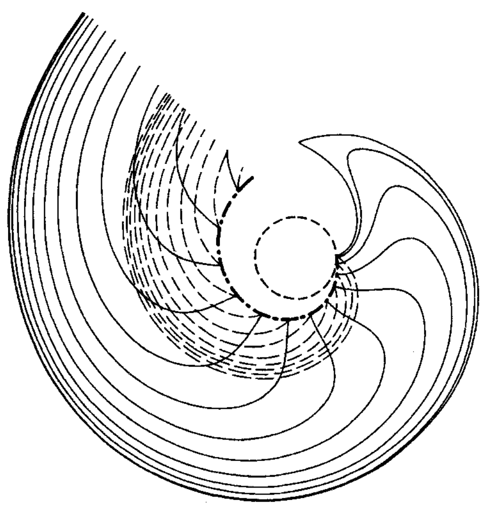

FIGURE 2. Cross-sections of the caustic (the envelope shown in figure 1) with a set of equidistant planes parallel to the plane of the orbit. The contours shown as broken lines belong to the sheet ϕ_+ of this surface which is here hidden underneath the sheet ϕ_-. The cusp curve – along which the two sheets of the caustic meet and are tangent to one another – is designated by dots and dashes, and the sonic cylinder by a broken circle. The two-sheeted, tube-like surface shown here is symmetric with respect to the plane of the orbit.

curve whose two segments run along the two sides of the spiralling tube-like surface from the point on the sonic cylinder where the cone becomes a tube to infinity. (See figure 2 and the figures in Lilley *et al.* 1953; da Costa & Kahn 1985; Ardavan 1989).

In the rectilinear case, the source points that influence the sound field at a given observation point P are only those that lie within an inverted Mach cone issuing from P (see figure 1 in Ardavan 1991*a*). What plays the role of the inverted Mach cone in the present case is a surface in the $(r, \hat{\varphi}, z)$-space of source points that has the same

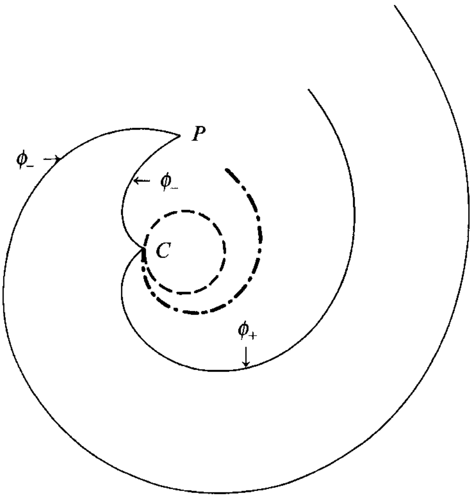

FIGURE 3. The bifurcation surface associated with a near-field observation point P. Only the cross-section of this surface with its plane of symmetry $z = z_P$ is shown. The curve designated by dots and dashes is the projection of the cusp curve of the bifurcation surface onto this plane. The different sheets, $\phi_\pm$, of the bifurcation surface are identified, and the sonic cylinder (the circle) and the point of tangency of the cusp curve with the sonic cylinder (point C) are also shown. When the observation point is placed in the far zone ($\hat{r}_P \gg 1$, $z_P \gg z$), the spiralling surface that issues from P undergoes a large number of turns – in which its two sheets intersect one another – before reaching the sonic cylinder. (The motion of the source is counterclockwise.)

shape and points in the same direction as the reflection of the caustic described above – which resides in the $(r_P, \hat{\varphi}_P, z_P)$-space of the observation points – across the meridional plane $\hat{\varphi} = \hat{\varphi}_P$ passing through its conical apex P. This surface, which is shown in figure 3, will be here referred to as the bifurcation surface associated with the observation point P. The source points lying inside this surface influence the field observed at its apex via waves that, though received simultaneously, were emitted at – at least – three different values of the retarded time, but the source points outside this surface influence the field via a single wave. The number of contributing retarded times can be more than three when the speed of the point source is appreciably greater than c (see da Costa & Kahn 1985). The points *on* the bifurcation surface approach the observer with the speed of sound along the radiation direction and so are sources of constructively interfering waves that not only arrive at P simultaneously but were emitted over a short time interval from one another, an interval in which the rates of change of their retarded times – as functions of the observation time – diverge. Amongst these, the points on the cusp curve (figure 4), which at the same time approach the observer with zero acceleration along the radiation direction, represent the source points for which the singularity of the spiral Green's function at P is worst, i.e. the focusing of the rays that form a caustic at P is sharpest.†

We shall demonstrate that the contributions towards the sound at any given point in the far zone that do not decay spherically are made by those source elements that, at the retarded time, were located in the vicinity of the cusp curve of the bifurcation

† In this paper we use the terminology of geometrical acoustics (rays, caustics, focusing, etc.) not in the narrow sense in which ray theory is an approximation to wave theory, but in the sense used by Courant & Hilbert (1962) and Friedlander (1958): certain aspects of the solutions to any second-order hyperbolic partial differential equation are described by the first-order partial differential equation (the eikonal equation) and the ordinary differential equations (the ray equations) which govern the characteristics and bicharacteristics of the original equation (see §6 of Ardavan 1989).

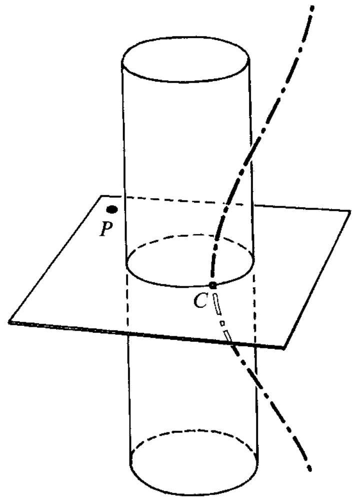

FIGURE 4. Position of the cusp curve of the bifurcation surface, designated by dots and dashes, in relation to those of the sonic cylinder $\hat{r} = 1$ and the symmetry plane $z = z_P$ for a near-field observation point P (schematic). The point C at which this cusp curve touches, and is tangent to, the sonic cylinder lies in the plane of symmetry containing P. As the observation point is moved towards the far-field, point C rotates through a large angle – of the order of $\hat{r}_P$ – about the sonic cylinder, and the segments of the cusp curve that lie away from C tightly wind around a second cylinder with the radius $\hat{r} = \operatorname{cosec} \theta_P$ (see (47) and (75)). (The motion of the source is counterclockwise.)

surface associated with that observation point (§§4 and 5). For this reason, we begin the presentation of our analysis by deriving an asymptotic approximation to the spiral Green's function at its caustic (the cusp curve of the bifurcation surface) both in the frequency and the time domains (§3). Each Fourier component of the spiral Green's function is given by an integral involving an exponential function (see equation (17) below) whose phase has two stationary points occurring on the two sheets of the bifurcation surface. Because these stationary points have positions that depend on the coordinates of the source point and coincide for source elements that lie on the cusp curve, the asymptotic expansion of the spiral Green's function cannot be obtained by the method of stationary phase; though generally applicable to cases in which the stationary points are isolated, this method does not yield a uniformly valid result in the range of parameters where the stationary points approach one another and coalesce. To handle the present problem, a more accurate technique is required in which the phase of the integral in question is transformed into a cubic function (cf. Chester, Friedman & Ursell 1957; Ludwig 1966; Bleistein & Handelsman 1986), rather than approximated by a quadratic one. The leading term in the resulting asymptotic expansion of the integral is then seen to arise from the locus at which the stationary points of the phase function coalesce.

A generalization of this technique (cf. Myers & Farassat 1987) also yields the asymptotic behaviour of the spiral Green's function at its caustic in the time domain (§3). The parameter, playing the role of wavelength, which should in this case approach zero for the expansion to hold is the distance of the source point from the cusp curve of the bifurcation surface (or the distance of the observation point from the cusp curve of the caustic surface).

To emphasize the role played by the source elements at the cusp curve of the bifurcation surface, we have based the asymptotic expansion of the sound field in the frequency domain (§4) on both the exact and the asymptotic forms of the spiral Green's function. This calculation shows that the leading term in the asymptotic expansion of the sound for large frequency (i.e. high harmonics of the rotation frequency ω) comes from a single point on the cusp curve of the bifurcation surface – point C in figure 4 – and is sharply beamed into the rotation plane containing the blade. It shows, moreover, that the leading contribution to the sound amplitude decays cylindrically, i.e. like $R_P^{-\frac{1}{2}}$, for values of R_P that do not exceed the Rayleigh distance, and has a spectrum that, in contrast to that of the emission from subsonic sources, falls off like $m^{-\frac{3}{2}}$ with the harmonic number m, rather than exponentially.

The fact that the range of validity of the calculation in §4 is limited by the requirement that the Rayleigh distance should exceed the distance of the observer from the source does not imply that the cylindrically decaying component of the radiation is composed of the higher harmonics of the rotation frequency exclusively. The condition on the Rayleigh parameter also appears when the decay rate of Mach waves from a finite-duration rectilinearly moving supersonic source is analysed in the frequency domain, whereas it is known from the time-domain analysis of the same problem that the cylindrical decay of Mach waves is independent of frequency (see Appendix A). In §5, we use the asymptotic expansion of the spiral Green's function at its caustic, in the time domain, to calculate the contribution towards the sound field of those source elements within the bifurcation surface that lie in the neighbourhood of one of the sheets of this surface, close to its cusp curve. The leading term in the resulting asymptotic expansion of the sound field confirms that not merely the high-frequency Fourier components of the sound, but the sound level itself, decays cylindrically, and that this result is a consequence solely of the behaviour of the spiral Green's function at its caustic – i.e. of the radiation efficiency of the volume elements of the source that approach the observer with the wave speed and zero acceleration along the radiation direction – rather than of any specific properties of the steady source distribution in the blade-fixed frame.

The component of the radiation whose amplitude decays like $R_P^{-\frac{1}{2}}$ is present at any observation point in the far zone for which the cusp curve of the bifurcation surface intersects the source distribution. From the shape of the cusp curve, it can thus be inferred that the latitudinal width of the radiation beam generated by a source distribution whose supersonic portion extends from the sonic cylinder to $r = r_0 > c/\omega$ is given by the range of angles satisfying cosec $\theta_P < r_0\,\omega/c$ (see §6). The longitudinal width of the overall radiation beam simply equals the longitudinal extent of the source distribution: a shift $\Delta\hat{\varphi}_P$ in the azimuthal position of any observation point results in an equal shift $\Delta\hat{\varphi}$ in the azimuthal position of the cusp curve associated with that observation point. Because, as we move away from the source, the area subtended by the solid angle into which this component of the radiation is beamed increases like R_P^2, while the flux density of the radiation decreases like R_P^{-1}, it might at first seem that the flux of energy is not the same across spheres of different radii enclosing the source. This apparent incompatibility with the conservation of energy, however, is resolved once we also take into account the fact that the emission time intervals associated with the volume elements of the source distribution that contribute towards this component of the radiation are by a large (R_P-dependent) factor greater than the time intervals during which the signals generated by these source elements are received.

For a point source that approaches the observer with the speed of sound along the radiation direction, a finite interval of retarded time is Doppler shifted to a vanishing interval of observation time. For those volume elements of an extended source that do not lie right on the bifurcation surface, the emitted wave fronts do not crowd together to such an extent that the ratio of the observation to the emission time intervals vanishes exactly. Nevertheless, the ratio in question has exceedingly small R_P-dependent values for the filamentary part of the source along the cusp curve of this surface that radiates coherently and so gives rise to the non-spherically decaying component of the radiation. The inverse square-root singularity of the leading term in the asymptotic expansion of the Green's function at its caustic – which arises from the vanishing of the Doppler factor in question – shows that for the source points neighbouring the cusp curve the ratio of the observation to the emission time intervals approaches zero like the square root of their distance from the bifurcation surface. When we integrate the Green's function over a neighbourhood of the cusp curve, we find that the contribution arising from its singularity introduces an extra factor of $R_P^{-\frac{1}{2}}$ into the expression for the sound strength that would have been absent had the Doppler factor been non-vanishing (§ 5).

The analysis itself makes it clear, therefore, that it is the Doppler contraction of the duration of the signal that is responsible for its cylindrical decay, i.e. for altering the R_P-dependence of its amplitude from R_P^{-1} to $R_P^{-\frac{1}{2}}$ (see equation (70) below). That the modifying factor should be $R_P^{-\frac{1}{2}}$, rather than R_P^{α} with a different value of α, is a consequence of the fact that the spiral Green's function has an inverse square-root singularity at its caustic (§ 3). In turn, that the spiral Green's function should have an inverse square-root singularity, as does the Green's function for a two-dimensional wave equation, is a consequence of the fact that the symmetry $\partial/\partial t = -\omega\,\partial/\partial\varphi$ reduces the spatial dimension of the wave equation that governs the present problem from three to two: the mathematical structure of the equation governing the present problem is precisely the same as that of the equation that governs (two-dimensional) axisymmetric waves in a non-homogeneous medium (§ 8).

Owing to the above symmetry, what is observed as a short-duration signal in the stationary inertial frame appears as a longitudinally narrow waveform in the blade-fixed rotating frame. The fact that the ratio of the observation to emission time intervals is smaller the further away we move from the source thus implies that the longitudinal width of the radiation beam that is generated by the filamentary locus of volume elements at the intersection of the cusp curve with the source distribution is narrower the larger R_P is. So, the requirements of the conservation of energy are met at this level by virtue of the fact that the enhancement of the flux density of energy at the position of the observer is compensated by a corresponding reduction in the size of the area subtended by the radiation beam of the individual filament which acts as a source (§ 6). This is essentially how the systems that generate non-spherically diverging isolated wave packets, known as acoustic or electromagnetic 'missiles' (Myers *et al.* 1990), conserve their energy (see also Ffowcs Williams & Guo 1988; Ffowcs Williams 1993*a*, *b*).

Because any change in the position of the observation point changes the segment along which the cusp curve of the bifurcation surface intersects the source distribution, the signals received at two neighbouring points in the blade-fixed frame arise from filaments that have both different extents and different strengths. The overall waveform received in the far zone thus consists of a continuous set of narrow 'spiky' signals (subpulses) with uneven and fluctuating amplitudes, whose pattern of subpulse structure changes radically as the distance R_P changes. Were it not for this fact, the results of §§ 5 and 6 would have suggested that volume-distributed sources should be regarded as the linear superposition of a (continuous) collection of independent filamentary sources each of which – in addition to emitting the ordinary spherically spreading radiation – generated a directed cylindrically decaying subpulse of diminishing duration. However, the filamentary sources in question do not – like ordinary sources – have an identity that is independent of the observation point and, in general, no two subpulses within the waveforms that are observed at different distances have identical filaments as their sources.

For this reason, the results of §§5 and 6 do not provide any information about the evolution of the subpulses of a waveform in the course of their propagation from the source to the observation point. They merely imply that the generated waveform is more 'spiky' the larger the distance at which it is observed. On the other hand, this feature alone suffices to explain how the solid angle occupied by the overall radiation beam remains independent of R_P without violating the conservation of energy. Even though the flux density of energy associated with a typical subpulse differs from its near-field value by the factor R_P^{-1}, the change in the microstructure of the waveform with increasing distance from the source alters the distribution of the flux density of energy over the cross-sectional area of the overall radiation beam in such a way that the integral of this flux density over the surface of a sphere enclosing the source becomes independent of R_P. That this should be so is dictated by the fact that the retarded solution of the wave equation, from which the cylindrical decay of the subpulses is derived, is manifestly compatible with the conservation of energy as far as the wave energy that is emitted by the entire source is concerned.

Section 7 of the paper is devoted to a discussion of the differences between the present results and those of the earlier works on rotor acoustics. A basic feature of published treatments of the present problem is that they are all based – in most cases implicitly – on various approximations to the expression for a Fourier component of the spiral Green's function. We have therefore begun in §7 by deriving the far-field and the high-frequency approximations to the spiral Green's function in the frequency domain, and comparing the resulting expressions to the leading term in the asymptotic expansion of this function at its caustic. Since the spiral Green's function is a discontinuous function, and so its spectrum extends to high harmonics of the rotation frequency, the sound amplitude that follows from the high-frequency approximation to this function is in fact identical to the cylindrically decaying amplitude predicted by the leading term in the asymptotic expansion of §4. The far-field limit of the high-frequency approximation to the spiral Green's function, however, misrepresents the site of emission: it implies that the main contribution to the high-frequency sound field in the far zone arises from the source elements on the cylindrical surface $r = c \operatorname{cosec} \theta_P/\omega$, rather than from the source elements on the cusp curve of the bifurcation surface which is a curve belonging to this cylinder.

When we introduce the far-field approximation first, we obtain an expression for the spiral Green's function that not only misrepresents the site of emission in the high-frequency limit, but in fact obliterates the non-spherically decaying component of the radiation altogether. The exact expression for the spiral Green's function (equation (7) below) involves a phase whose two nearby stationary points coalesce as the source point approaches the cusp curve of the bifurcation surface. In the far-field approximation, this phase function is replaced by the first two terms in its Taylor expansion in powers of $|\boldsymbol{x}|/|\boldsymbol{x}_P|$, where $\boldsymbol{x}$ and $\boldsymbol{x}_P$ are the position vectors of the source point and the observation point, respectively. Unless some of the higher-order terms in this Taylor expansion are also retained, however, the resulting expression would not be an exact enough representation of the phase of the spiral Green's function for the effects described in this paper to show up. To extract the cylindrically decaying component of the radiation, whose existence is intimately connected with the focusing of rays and so the coalescing of the stationary points of the phase function in question, it is essential that the phase of the integrand in the integral defining the spiral Green's function is (as in §3) transformed into, or at least approximated by, a cubic function of the variable over which it extends, and that the coefficients of this cubic function are only simplified by means of approximations that remain uniformly valid at the source points where its extrema coalesce (see §7). Because the present problem entails the formation of caustics, its analysis requires a more exact solution of the wave equation than that supplied by the far-field approximation to the retarded potential; to base the analysis on such a solution is simply tantamount to limiting the type of phenomena that can be described.

It is, in addition, essential that account is taken of the contribution from the volume distribution of quadrupole sources; none of the features described above can, in general, appear in the radiation from surface source distributions (§8). In §8 we also briefly comment on the practical implications of the paper's results and point out how the breaking of the symmetry of the flow can, in principle, suppress the noise in the far zone.

2. Formulation of the problem: the spiral Green's function

The generation of sound by a rigid body in arbitrary motion through a fluid is governed by the following wave equation, known as the Ffowcs Williams–Hawkings equation, which is an exact consequence of the conservation laws for mass and momentum:

$$\nabla^2\rho - \frac{1}{c^2}\frac{\partial^2 \rho}{\partial t^2} = -4\pi s, \tag{1}$$

with
$$s = \frac{1}{4\pi c^2}\left\{\frac{\partial^2}{\partial x_i\,\partial x_j}[T_{ij}\,\theta(f)] - \frac{\partial}{\partial x_i}\left[p_{ij}\frac{\partial}{\partial x_j}\delta(f)\right] + \frac{\partial}{\partial t}\left[\rho_0 v_i \frac{\partial f}{\partial x_i}\delta(f)\right]\right\} \tag{2}$$

where ρ and p_{ij} are the deviations of the density and the stress tensor of the ambient fluid from their mean values ρ_0 and $p_0\,\delta_{ij}$, the constant c is the mean value of the speed of sound, $\boldsymbol{v}$ is the local velocity with which the surface of the body encroaches on the fluid, and $f(\boldsymbol{x}, t) = 0$ defines the surface of the moving body with $f < 0$ inside and $f > 0$ outside the body. The tensor $T_{ij} = (\rho_0 + \rho)\,u_i\,u_j + p_{ij} - \rho c^2 \delta_{ij}$, in which $\boldsymbol{u}$ stands for the fluid velocity, is Lighthill's stress tensor. In these expressions $\boldsymbol{x}$ is the position vector, t is time, $\theta(f)$, $\delta(f)$ and δ_{ij} are the Heaviside step function and the Dirac and Kronecker delta functions, respectively, and the indices i and j designate Cartesian components of tensors that are to be summed over the values 1, 2 and 3 when repeated.

Equation (1) is a nonlinear equation because, even though the source term in this equation is known to within the zeroth order in the perturbation quantities, a knowledge of the exact value of s requires knowledge of the flow field and so of the solution itself. Nevertheless, it is possible to use the retarded Green's function for the linear wave equation in unbounded space to rewrite (1) formally as

$$\rho(\boldsymbol{x}_P, t_P) = \int \mathrm{d}^3x\,\mathrm{d}t\, s(\boldsymbol{x}, t)\,\delta(t - t_P + R/c)/R, \tag{3}$$

where $(\boldsymbol{x}_P, t_P)$ and $(\boldsymbol{x}, t)$ denote the coordinates of the observation and the source points, respectively, R stands for $|\boldsymbol{x} - \boldsymbol{x}_P|$, and the integral extends over all space-time.

When the body in question is a hovering blade with no forward velocity and its motion consists of a rigid rotation about a fixed axis with a constant angular frequency ω, the quasi-steady sources of sound whose strengths do not vary with time in the blade-fixed coordinates are thought to be most important (see Hawkings & Lowson

1974), and we are concerned with flow variables which depend on the azimuthal angle φ and the time t as functions of the single variable $\varphi-\omega t$. Thus for that part of rotor acoustics, in which ρ, f and the cylindrical components of $\boldsymbol{u}$, $\boldsymbol{v}$ and p_{ij} possess the symmetry $\partial/\partial t+\omega\,\partial/\partial\varphi=0$, the source term of (1) has the form

$$\left.\begin{aligned} s(r,\varphi,z,t) &= s(r,\hat{\varphi},z), \\ \hat{\varphi} &\equiv \varphi-\omega t, \end{aligned}\right\} \tag{4}$$

where the z-axis of the cylindrical polar coordinates (r,φ,z) is defined by the axis of rotation. (This can be seen by transforming the partial derivatives with respect to the Cartesian coordinates that appear in (2) into covariant derivatives with respect to cylindrical coordinates, and noting that the process of differentiation does not introduce any dependence on the individual variables φ or t.)

If we now insert (4) in (3), write R in its cylindrical form

$$R = [(z-z_P)^2+r^2+r_P^2-2rr_P\cos(\varphi-\varphi_P)]^{\frac{1}{2}}, \tag{5}$$

and change the variables of integration from (r,φ,z,t) to $(r,\varphi,z,\hat{\varphi})$, the sound amplitude becomes

$$\rho(r_P,\hat{\varphi}_P,z_P) = \int r\,\mathrm{d}r\,\mathrm{d}\hat{\varphi}\,\mathrm{d}z\,s(r,\hat{\varphi}\,z)\,G_0(r_P,\hat{\varphi}_P,z_P;r,\hat{\varphi},z), \tag{6}$$

in which

$$G_0 \equiv \oint \mathrm{d}\varphi\,\delta(\hat{\varphi}_P-\hat{\varphi}+\varphi-\varphi_P+R\omega/c)/R \tag{7}$$

$$= \sum_{\varphi=\varphi_j} \frac{1}{R|\mathrm{d}g/\mathrm{d}\varphi|} \tag{8}$$

plays the role of an effective Green's function (the so-called spiral Green's function). Here, the integration with respect to $\hat{\varphi}$ is over $-\infty<\hat{\varphi}<+\infty$, and the angles φ_j – which correspond to the retarded times at which the source point $(r,\hat{\varphi},z)$ makes its contribution towards the value of G_0 at the observation point $(r_P,\hat{\varphi}_P,z_P)$ – are solutions of the transcendental equation

$$g(\varphi) \equiv \varphi-\varphi_P+R\omega/c = \hat{\varphi}-\hat{\varphi}_P \equiv \phi \tag{9}$$

in the range $-\pi<\varphi-\varphi_P<\pi$. (The present $g(\varphi)$ is the same as $g(\frac{1}{2}\varphi-\frac{1}{2}\varphi_P+\frac{1}{2}\pi)$ of Ardavan 1989.)

When $r\omega \geqslant c$, i.e. the speed of the source point equals or exceeds the speed of the waves it generates, $g(\varphi)$ is an oscillatory function of φ whose derivative vanishes at

$$\varphi_\pm = \varphi_P-\arcsin(\hat{r}_P^{-1}\hat{r}^{-1}h_\pm), \tag{10}$$

and the Green's function G_0 diverges on the following two-sheeted surface at which $\mathrm{d}g/\mathrm{d}\varphi=0$:

$$\phi = \phi_\pm \equiv h_\pm-\arcsin(\hat{r}_P^{-1}\hat{r}^{-1}h_\pm). \tag{11}$$

Here,

$$h_\pm \equiv [(\hat{z}-\hat{z}_P)^2+\hat{r}^2+\hat{r}_P^2-2\pm 2\Delta^{\frac{1}{2}}]^{\frac{1}{2}}, \tag{12}$$

where

$$\Delta \equiv (\hat{r}_P^2-1)(\hat{r}^2-1)-(\hat{z}-\hat{z}_P)^2, \tag{13}$$

and $(\hat{r},\hat{z};\hat{r}_P,\hat{z}_P)$ stand for the dimensionless coordinates $r\omega/c$, $z\omega/c$, $r_P\omega/c$ and $z_P\omega/c$, respectively. The two sheets ($\pm$) of the tube-like spiralling surface $\phi=\phi_\pm$ are tangent to one another and form a cusp along the curve

$$\phi = (\hat{r}_P^2\hat{r}^2-1)^{\frac{1}{2}}-\arctan(\hat{r}_P^2\hat{r}^2-1)^{\frac{1}{2}}, \tag{14a}$$

$$\hat{z}-\hat{z}_P = \pm(\hat{r}_P^2-1)^{\frac{1}{2}}(\hat{r}^2-1)^{\frac{1}{2}}, \tag{14b}$$

where they meet. On this cusp curve, $\mathrm{d}^2 g/\mathrm{d}\varphi^2$ also vanishes and the Green's function G_0 has a higher-order singularity.

When the source point $(r, \hat{\varphi}, z)$ is fixed and (11) describes a surface in the $(r_P, \hat{\varphi}_P, z_P)$-space of the observation points, we call this surface – which constitutes the envelope of the wave fronts emanating from the source point in question – the caustic (see figures 1 and 2).† But when the observation point is fixed and (11) describes a surface in the $(r, \hat{\varphi}, z)$-space, we refer to it as the bifurcation surface. The bifurcation surface in the $(r, \hat{\varphi}, z)$-space has the same shape and points in the same direction as the surface that is obtained by reflecting the caustic across the meridional plane $\hat{\varphi}_P = \hat{\varphi}$ in the $(r_P, \hat{\varphi}_P, z_P)$-space. Figure 3 shows the bifurcation surface associated with an observation point in the near field, and figure 4 is a schematic sketch of the position of the cusp curve of a bifurcation surface in relation to that of the sonic cylinder $\hat{r} = 1$. For $\hat{r}_P \gg 1$, (14*a*) yields $\mathrm{d}\phi/\mathrm{d}\hat{r} \approx \hat{r}_P$, which means that the cusp curve of the bifurcation surface associated with an observation point in the far zone winds around the sonic cylinder through a large angle – of the order of $\hat{r}_P$ – before advancing a short distance in $\hat{r}$.

When we superpose the sound waves from the volume elements that constitute an extended source, as in the expression for $\rho(r_P, \hat{\varphi}_P, z_P)$ in (6), the coordinates of the observation point $(r_P, \hat{\varphi}_P, z_P)$ are fixed and we are primarily concerned with the behaviour of the Green's function G_0 which appears in the integrand of this equation as a function of the coordinates $(r, \hat{\varphi}, z)$ of the source point. Just as in the case of a rectilinearly moving source distribution where the source points that produce an infinite sound at a given observation point P are those that lie on the inverted Mach cone issuing from P (see figure 1 in Ardavan 1991*a*), so in the present case the singularity of G_0 in the $(r, \hat{\varphi}, z)$-space occurs on the bifurcation surface. In other words, the present bifurcation surface is simply the counterpart of what in the rectilinear case appears as an inverted Mach cone (see figure 2 in Ardavan 1991*a*).

The bifurcation surface divides the volume of the source into two parts with differing influences on the field; whereas the source elements outside this surface influence the sound field observed at its conical apex, P, at only a single instant, the source elements inside the surface influence this field at three values of the retarded time. For source points *on* the bifurcation surface, which approach the observation point P with the wave speed along the radiation direction, the values of two of the three retarded times in question coincide and the wavelets that arrive at P interfere constructively to form a singularity. In the case of a source point that lies on the *cusp curve* of the bifurcation surface, i.e. that approaches the observer with zero acceleration as well as with the wave speed along the radiation direction‡ the singularity of G_0 is caused by the coincidence of all three values of the retarded time and is therefore of a higher order. (The physical content of the introductory material presented in this section, which forms the basis of the following analysis, has been discussed in detail in Ardavan 1989, 1991*a*.)

† Note that the caustic is here defined as the envelope of the wave fronts emanating from a circularly moving point source, without any reference to frequency.

‡ From (5), (9) and $\varphi = \omega t + \hat{\varphi}$, it can be seen that the equation $\mathrm{d}g/\mathrm{d}\varphi = 0$, which defines the bifurcation surface, is equivalent to

$$\left.\frac{\mathrm{d}R}{\mathrm{d}t}\right|_{t=t_P-R/c} = c,$$

and the equation $\mathrm{d}^2 g/d\varphi^2 = 0$, defining the cusp curve of this surface, is equivalent to

$$\left.\frac{\mathrm{d}^2 R}{\mathrm{d}t^2}\right|_{t=t_P-R/c} = 0.$$

3. Asymptotic expansion of the spiral Green's function at its caustic

It is not possible to solve (9) explicitly and so find an exact expression for the Green's function G_0. However, we shall see in the following sections that the non-spherically decaying contribution towards the value of ρ at a given observation point within the solid angle (76) is in fact made by the source elements in the vicinity of the cusp curve of the bifurcation surface that is associated with that observation point. What is needed for the purposes of the present analysis, therefore, is only an asymptotic approximation to G_0 in the neighbourhood of the cusp curve (14), an approximation that easily follows from the method already developed by Chester *et al.* (1957) and Ludwig (1966).

Since the source density $s(r, \hat{\varphi}, z)$ is a periodic function of the azimuthal coordinate $\hat{\varphi}$ of the blade-fixed frame, it can be expanded into a Fourier series. Insertion of this series in (6), in turn, results in the Fourier representation

$$\rho = \sum_{m=-\infty}^{\infty} e^{im\hat{\varphi}_P} \int r\,dr\,dz\, s_m \hat{G}_{0m}, \tag{15}$$

where

$$s_m \equiv (2\pi)^{-1} \int_{-\pi}^{\pi} d\hat{\varphi}\, e^{-im\hat{\varphi}} s, \tag{16}$$

and

$$\hat{G}_{0m} \equiv \oint \frac{d\varphi}{R} e^{img(\varphi)}. \tag{17}$$

We are concerned in this section with asymptotic approximations both to the Fourier component $\hat{G}_{0m}$, and to the Green's function G_0 itself.

As long as the observation point does not coincide with the source point, the function $g(\varphi)$ is analytic (see Ardavan 1989) and the following transformation of the integration variable in (17) is permissible:

$$g(\varphi) = \tfrac{1}{3}\nu^3 - a^2\nu + b, \tag{18}$$

where ν is the new variable of integration, and the constants

$$a \equiv (\tfrac{3}{4})^{\frac{1}{3}}(\phi_+ - \phi_-)^{\frac{1}{3}} \quad \text{and} \quad b \equiv \tfrac{1}{2}(\phi_+ + \phi_-) \tag{19}$$

are chosen such that the values of the two functions on opposite sides of (18) coincide at their extrema (cf. (11)). Thus an alternative exact expression for $\hat{G}_{0m}$, within the region $\Delta > 0$ where $\phi_\pm$ are well-defined, is

$$\hat{G}_{0m} = \int d\nu\, I \exp[im(\tfrac{1}{3}\nu^3 - a^2\nu + b)],$$

in which

$$I \equiv R^{-1}\, d\varphi/d\nu, \tag{21}$$

and the range of integration is the image of $-\pi < \varphi - \varphi_P < \pi$ under the mapping (18).

Now, close to the cusp curve of the bifurcation surface at which a vanishes and the extrema $\nu = \pm a$ of the above cubic function coalesce, I may be approximated by

$$I_0 = p + q\nu, \tag{22}$$

where

$$p = \tfrac{1}{2}(I|_{\nu=a} + I|_{\nu=-a}), \tag{23}$$

and

$$q = \tfrac{1}{2}a^{-1}(I|_{\nu=a} - I|_{\nu=-a}). \tag{24}$$

The resulting expression for $\hat{G}_{0m}$ will then constitute, according to the general theory described in Bleistein & Handelsman (1986, chapter 9), the leading term in the asymptotic expansion of this quantity for large (positive) m. Equations (18) and (21) yield a function I which is indeterminate at $\nu = \pm a$. Using l'Hopital's rule and the solutions (10) of $\mathrm{d}g/\mathrm{d}\varphi = 0$, we find, from (23) and (24), that

$$p = (\omega/c)\,(\tfrac{1}{2}a)^{\frac{1}{2}}(h_-^{-\frac{1}{2}} + h_+^{-\frac{1}{2}})\,\Delta^{-\frac{1}{4}}, \tag{25}$$

and

$$q = (\omega/c)\,(2a)^{-\frac{1}{2}}(h_-^{-\frac{1}{2}} - h_+^{-\frac{1}{2}})\,\Delta^{-\frac{3}{4}}. \tag{26}$$

These expressions are, in turn, indeterminate on the cusp curve, but their limiting values,

$$p_0 \equiv p|_{\Delta=0} = 2^{\frac{1}{3}}(\omega/c)\,(\hat{r}_P^2\hat{r}^2 - 1)^{-\frac{1}{2}}, \tag{27}$$

$$q_0 \equiv q|_{\Delta=0} = 2^{-\frac{1}{3}}(\omega/c)\,(\hat{r}_P^2\hat{r}^2 - 1)^{-1}, \tag{28}$$

on this curve are both finite and non-zero.

Not only can I in (20) be written as I_0, but also the integration limits in this equation can be replaced with $\pm\infty$ without altering the value of the leading term in its asymptotic expansion. Hence, for a large positive m we obtain

$$\hat{G}_{0m} \sim 2\pi m^{-\frac{1}{3}} \mathrm{e}^{imb}[p\mathrm{Ai}(-m^{\frac{2}{3}}a^2) - im^{-\frac{1}{3}}q\mathrm{Ai}'(-m^{\frac{2}{3}}a^2)] \tag{29}$$

by virtue of the definition of the Airy function. (The corresponding value of $\hat{G}_{0m}$ for negative m is given by the complex conjugate of the right-hand side of (29).) This expression, which though indeterminate is finite on the cusp curve, represents the leading term of an asymptotic expansion that is uniform with respect to the parameter Δ, and includes the expression that is obtained by the method of stationary phase as a special case (see §6). Note that the term involving the derivative of an Airy function in (29) is smaller than the first term in this equation by a factor that vanishes like R_P^{-1} for $R_P = (r_P^2 + z_P^2)^{\frac{1}{2}} \to \infty$, and like $m^{-\frac{1}{3}}$ for $m \to \infty$ when $\Delta = 0$.

The above expansion can in fact be carried out also in the time domain. Because the high-frequency contributions ($m \gg 1$) to the Fourier transform of G_0 are received from the discontinuity on the cusp curve of the bifurcation surface where this function is most singular, the expansion of $\hat{G}_{0m}$ for large m in the frequency domain corresponds to a special case of the expansion of G_0 at its cusp curve in the time domain, i.e. to a limited regime of the same approximation.†

To obtain the expansion in the time domain, we only need to use (18) and (21) to rewrite (7) as

$$G_0 = \int \mathrm{d}\nu\, I\delta(\tfrac{1}{3}\nu^3 - a^2\nu + b - \phi), \tag{30}$$

and replace I by I_0; then the integral, whose limits should also be replaced by $\pm\infty$, can be evaluated explicitly. Depending on whether the cubic equation for ν, which follows from the vanishing of the argument of the delta-function in (30), has three roots or one root, the result is

$$G_0 \sim 2a^{-2}(1-\chi^2)^{-\frac{1}{2}}[p\cos(\tfrac{1}{3}\arcsin\chi) - aq\sin(\tfrac{2}{3}\arcsin\chi)], \quad |\chi| < 1, \tag{31a}$$

or

$$G_0 \sim a^{-2}(\chi^2-1)^{-\frac{1}{2}}[p\sinh(\tfrac{1}{3}\operatorname{arccosh}|\chi|) + aq\operatorname{sgn}(\chi)\sinh(\tfrac{2}{3}\operatorname{arccosh}|\chi|)], \quad |\chi| > 1, \tag{31b}$$

where

$$\chi \equiv [\phi - \tfrac{1}{2}(\phi_+ + \phi_-)]/[\tfrac{1}{2}(\phi_+ - \phi_-)]. \tag{32}$$

† Note that what we have here called the cusp curve is in the discussion of the general theory given by Ludwig (1966) referred to as the caustic. From the point of view of the lower-dimensional $(r, \hat{\varphi}, z)$-space in which (1) reduces to an equation of the mixed type, i.e. to (82), the bifurcation surface is the ray conoid of the governing equation in its domain of hyperbolicity, and the cusp curve is the locus of the points at which the rays focus and form a caustic (see Ardavan 1989, §6, and Ardavan 1991*a*, §3).

Once again, the second terms in (31 a) and (31 b) are smaller than the first terms in these equations by a factor that vanishes like R_P^{-1} as $R_P \to \infty$. The corresponding expression for G_0 outside the region $\Delta > 0$, where there is no caustic, is not in fact needed for the following analysis.

4. Asymptotic expansion of the radiation field in the frequency domain

To calculate the asymptotic values of the coefficients in the Fourier representation of the sound field of an extended source, we must now insert (29) in (15) and carry out the remaining integrations over the volume of the source. We shall however begin the analysis in this section with the exact expression (20) for G_{0m}, rather than with (29), in order to emphasize the role played by the source elements at the cusp curve of the bifurcation surface in the generation of the leading contribution to the sound field.

The variables a and b that appear in (20) may be expressed as functions of r and z, with the aid of (19), by noting that according to (11) and (12), we have

$$h_\pm = \xi_+ \pm \xi_-, \tag{33}$$

and hence

$$\tfrac{1}{2}(\phi_+ \pm \phi_-) = \xi_\pm - \arctan \xi_\pm, \tag{34}$$

where

$$\xi_\pm \equiv \{\tfrac{1}{2}(\zeta^2 + \hat{r}^2 + \hat{r}_P^2 - 2) \pm \surd[\tfrac{1}{4}(\zeta^2 + \hat{r}^2 + \hat{r}_P^2 - 2)^2 - \Delta]\}^{\frac{1}{2}}, \tag{35}$$

$$\zeta \equiv \hat{z} - \hat{z}_P, \tag{36}$$

and Δ is defined in (13). In the present case, a pair of independent variables, more suitable than (r, z) for marking the points inside the region $\Delta = \xi_-^2\,\xi_+^2 > 0$, is ξ_-, which vanishes on the cusp curve, and ζ. If we use (35) and (36) to replace r and ξ_+ everywhere by

$$\hat{r} = (1 + \xi_-^2)^{\frac{1}{2}}[1 + \zeta^2(\hat{r}_P^2 - 1 - \xi_-^2)^{-1}]^{\frac{1}{2}}, \tag{37}$$

$$\xi_+ = [\hat{r}_P^2 - 1 + \hat{r}_P^2\zeta^2(\hat{r}_P^2 - 1 - \xi_-^2)^{-1}]^{\frac{1}{2}}, \tag{38}$$

and note that the transformation from (r, z) to (ξ_-, ζ) has the Jacobian

$$\partial(\hat{r}, \hat{z})/\partial(\xi_-, \zeta) = \hat{r}^{-1}\xi_-[1 + \hat{r}_P^2\,\zeta^2(\hat{r}_P^2 - 1 - \xi_-^2)^{-2}], \tag{39}$$

we find that (15) and (20) jointly yield

$$\rho = \sum_{m=-\infty}^{+\infty} \rho_m\, \mathrm{e}^{\mathrm{i}m\varphi_P}, \tag{40}$$

with

$$\rho_m \equiv (c/\omega)^3 \int \mathrm{d}\nu\, \mathrm{d}\zeta\, \mathrm{d}\xi_-\, \xi_-\, s_m\, I[1 + \hat{r}_P^2\zeta^2(\hat{r}_P^2 - 1 - \xi_-^2)^{-2}] \times \exp\{im[\tfrac{1}{3}\nu^3 - (\tfrac{3}{2})^{\frac{2}{3}}(\xi_- - \arctan \xi_-)^{\frac{2}{3}}\nu + \xi_+ - \arctan \xi_+]\}, \tag{41}$$

in which ξ_+ is to be regarded as the function of (ξ_-, ζ) given in (38).

Because the phase of the integrand in (41) is stationary at $\xi_- = 0$, $\nu = 0$, for any given ζ, it now follows that the main contributions towards the value of the ξ_--quadrature are made by the source elements at the cusp curve, and that we may approximate both the phase and the amplitude in this equation by their values in the neighbourhood of $\xi_- = 0$. Thus replacing I by I_0 (as in (22)–(24)), evaluating I_0 at $\xi_- = 0$ (as in (27) and (28)), and neglecting the smaller term proportional to q_0, we find that the integration over ν results in

$$\rho_m \sim 2\pi(c/\omega)^2(\tfrac{1}{2}m)^{-\frac{1}{3}}(\hat{r}_P^2 - 1)^{-1} \int \mathrm{d}\zeta\, \mathrm{d}\xi_-\, \xi_-\, \xi_0\, s_m|_{\xi_-=0} \times \mathrm{Ai}[-(\tfrac{1}{2}m)^{\frac{2}{3}}\xi_-^2]\exp[im(\xi_0 - \arctan \xi_0)], \tag{42}$$

where $$\xi_0 \equiv \xi_+|_{\xi_-=0} = [\hat{r}_P^2 - 1 + \hat{r}_P^2(\hat{r}_P^2-1)^{-1}\zeta^2]^{\frac{1}{2}}. \tag{43}$$

This equation is in fact a direct consequence also of (15), (29) and (40).

The integration with respect to ξ_- in (42) extends, according to the method of stationary phase, over $(0, \infty)$, which comprises all permissible values of ξ_-, and may be performed immediately:

$$\int_0^\infty \mathrm{d}\xi_-\, \xi_-\, \mathrm{Ai}[-(\tfrac{1}{2}\mathrm{m})^{\frac{2}{3}}\xi_-^2] = \tfrac{1}{3}(\tfrac{1}{2}m)^{-\frac{2}{3}} \tag{44}$$

(see formulae (10.4.35) and (11.4.17) of Abramowitz & Stegun 1970). Combining (42) and (44), we obtain

$$\rho_m \sim 4\pi(c/\omega)^2[3m(\hat{r}_P^2-1)]^{-1}\int \mathrm{d}\zeta\, s_m|_{\xi_-=0}\,\xi_0 \exp[\mathrm{i}m(\xi_0 - \arctan\xi_0)]. \tag{45}$$

The phase of the integrand in the remaining integral in (45) is stationary at $\zeta = 0$, so that the leading contribution towards the value of the ζ-quadrature is given by

$$\rho_m \sim \tfrac{4}{3}\pi(c/\omega)^2 m^{-1}(\hat{r}_P^2-1)^{-\frac{1}{2}}\exp(\mathrm{i}m\phi_C)\int \mathrm{d}\zeta\, s_m|_{\xi_-=0}\exp[\tfrac{1}{2}\mathrm{i}m(\hat{r}_P^2-1)^{-\frac{1}{2}}\zeta^2], \tag{46}$$

in which $$\phi_C \equiv (\hat{r}_P^2-1)^{\frac{1}{2}} - \arctan(\hat{r}_P^2-1)^{\frac{1}{2}}. \tag{47}$$

Provided that the Fourier component $s_m|_{\xi_-=0}$ of the source density along the cusp curve has a support l in z for which the Rayleigh distance $m\omega l^2/c$ is much greater than $(1-\hat{r}_P^{-2})^{\frac{1}{2}}r_P$, and has a lengthscale of variation l' for which $m\omega l'/c$ is much smaller than unity, we may now replace the interval of integration by $(-\infty, +\infty)$ and the amplitude of the integrand, $s_m|_{\xi_-=0}$, by $s_m|_{\xi_-=0,\zeta=0}$ to reduce the integral in (46) to a Fresnel integral whose value is known (formulae (7.3.20) of Abramowitz & Stegun 1970):

$$\rho_m \sim \tfrac{2}{3}(c/\omega)^2(2\pi/m)^{\frac{3}{2}}(\hat{r}_P^2-1)^{-\frac{1}{4}}\exp[\mathrm{i}(m\phi_C + \tfrac{1}{4}\pi)]\, s_m|_{\xi_-=0,\zeta=0}. \tag{48}$$

This contribution, which comprises the leading term in the asymptotic expansion of ρ_m for large m, thus arises from the vicinity of a single source point at the intersection of the cusp curve and the sonic cylinder (point C in figure 4), and is detectable only in the orbital planes of the volume elements which constitute the source distribution, i.e. over an interval in z_P which equals the z-extent of the source distribution. What distinguishes point $C(\hat{r} = 1, \zeta = 0, \phi = \phi_C)$ from the other points on the cusp of the bifurcation surface is that not only does a source element located at this point move with the wave speed and zero acceleration relative to the observer, but it also has a velocity whose magnitude (and not just its component along the radiation direction) equals the speed of sound.

As long as the source density s has non-zero Fourier components at high enough harmonics of the rotation frequency ($m \gg 1$) for the Rayleigh distance to be greater than the distance of the observer from the source, it follows from (48) that the corresponding Fourier components ρ_m of the sound amplitude, and hence ρ itself, would fall off like $\hat{r}_P^{-\frac{1}{2}}$ with the distance $\hat{r}_P(\gg 1)$ away from the source. This is a property that the present type of radiation shares with the better known Mach emission from a rectilinearly moving supersonic source. But for Mach emission by a finite-duration source, it is known from an analysis in the time domain (see Appendix A) that the sound amplitude falls off cylindrically, i.e. like $r_P^{-\frac{1}{2}}$, whatever the Rayleigh distance relative to the distance r_P of the observer from the path of the source may be. One would expect, therefore, that as in the rectilinear case the non-spherical decay of the sound amplitude is a frequency-independent feature of the present radiation that remains in force irrespective of whether or not s_m is non-zero for large m. The time-domain calculation in the following section in fact confirms this expectation.

5. Asymptotic expansion of the radiation field in the time domain

The sound field arising from each supersonically moving constituent point of the source diverges on the caustic associated with that source point and decays spherically outside this surface. The singularity on the caustic is due to the infinite density of a point source and is removed once the fields of a continuous set of point sources are superposed, i.e. once the Green's function G_0 is convolved with the source density over the volume of an extended source (see Ardavan 1991*a*). However, since there is a possibility of constructive interference between the contributions from different source elements, which is mathematically reflected in the divergence of the Green's function on the bifurcation surface of a given observation point, the resulting singularity-free field of an extended source need not decay like R_P^{-1} when R_P tends to infinity along the associated caustics. In this section, we show that this is in fact so by calculating the contributions of the source elements located on the cusp curve of the bifurcation surface from (6) – for an arbitrary source density – directly in the time domain. The cylindrical decay of sound encountered in the above frequency-domain analysis is thus seen to be a feature that pertains to all harmonics of the rotation frequency that enter the Fourier decomposition of the radiation.

Right on the cusp curve of the bifurcation surface, the variables $\xi_\pm$ which were introduced in (35) assume the values

$$\xi_-|_{\Delta=0} = 0 \tag{49}$$

and

$$\xi_+|_{\Delta=0} \equiv \xi_0 = (\hat{r}_P^2\hat{r}^2 - 1)^{\frac{1}{2}}, \tag{50}$$

if we parametrize the cusp curve by $\hat{r}$, rather than by $\hat{z}$ as in (43). So, in the neighbourhood of this curve, i.e. for $\xi_- \ll 1$, we have

$$h_\pm \approx \xi_0, \tag{51}$$

$$b \approx \xi_0 - \arctan\xi_0, \tag{52}$$

$$a \approx (\tfrac{3}{2})^{\frac{1}{3}}(\xi_- - \arctan\xi_-)^{\frac{1}{3}} \approx 2^{-\frac{1}{3}}\xi_-, \tag{53}$$

$$\Delta \approx \xi_0^2\xi_-^2, \tag{54}$$

where use has been made of (19) and (33)–(35). The corresponding values of p and q are

$$[p, q] \approx 2^{\frac{1}{3}}(\omega/c)\,\xi_0^{-\frac{1}{2}}[1, 4^{-\frac{1}{3}}\xi_0^{-\frac{1}{2}}], \tag{55}$$

which were derived in (27) and (28).

The variable χ that appears in expression (31) for the asymptotic value of the Green's function equals ± 1 on the bifurcation surface: it has the value $+1$ on the sheet $\phi = \phi_+$ and the value -1 on the sheet $\phi = \phi_-$. On the cusp curve of the bifurcation surface, however, both the numerator and the denominator in (32) vanish, so that the value of χ depends on the direction along which this curve is approached. In the neighbourhood of the cusp curve, we have

$$\chi \approx (\phi - \xi_0 + \arctan\xi_0)/(\tfrac{2}{3}a^3), \tag{56}$$

in which

$$a \approx 2^{-\frac{1}{3}}\Delta^{\frac{1}{2}}\xi_0^{-1}, \tag{57}$$

and

$$\Delta \approx 2(\hat{r}_P^2 - 1)^{\frac{1}{4}}(\hat{r}^2 - 1)^{\frac{1}{4}}[(\hat{r}_P^2 - 1)^{\frac{1}{2}}(\hat{r}^2 - 1)^{\frac{1}{2}} - |\zeta|]. \tag{58}$$

(See equations (52)–(54), (32) and (13).)

If in addition to being close to the cusp curve of the bifurcation surface – which spirals out to infinity – the observation point is located in the far zone, i.e. $\hat{r}_P \gg 1$, then the variable ξ_0 defined in (50) reduces to $\hat{r}\hat{r}_P$ and hence (55) becomes

$$[p, q]_{\Delta=0, \hat{r}_P \to \infty} = 2^{\frac{1}{3}}(\omega/c)(\hat{r}\hat{r}_P)^{-1}[1, 4^{-\frac{1}{3}}(\hat{r}\hat{r}_P)^{-\frac{2}{3}}]. \tag{59}$$

Also, (57) and (58) show that a approaches the value

$$a|_{\Delta\to 0, \hat{r}_P\to\infty} = 2^{\frac{1}{6}}(1-\hat{r}^{-2})^{\frac{1}{4}}[(1-\hat{r}^{-2})^{\frac{1}{2}} - (\hat{r}\hat{r}_P)^{-1}|\zeta|]^{\frac{1}{2}}, \tag{60}$$

which is independent of the radial distance $\hat{R}_P\,(\gg 1)$ of the observer from the source: the fact that $z_P = R_P \cos\theta_P \gg z$ when the source is localized about $z = 0$ and $\theta_P \neq \frac{1}{2}\pi$ implies that $\hat{r}_P^{-1}|\zeta|$ tends to $\cot\theta_P$ for all values of the colatitude

$$\theta_P \equiv \arccos(z_P/R_P). \tag{61}$$

Thus it follows from (60) and (61) that, in the radiation zone, the terms involving q in expressions (31) for the Green's function, that decay faster than R_P^{-1}, must be neglected.

For source points that lie within the bifurcation surface, and an observation point that is located in the far zone, therefore, the asymptotic value of the Green's function G_0 at its caustic is given by the first term in (31a). If we introduce the following two variables which vanish on the cusp curve of the bifurcation surface:

$$\tilde{\phi} \equiv \phi - \xi_0 + \arctan\xi_0, \tag{62}$$

$$\tilde{\zeta} \equiv \hat{r}_P(\hat{r}^2-1)^{\frac{1}{2}} - |\zeta| \tag{63}$$

(cf. (14) for $\hat{r}_P \gg 1$), then the expression for this asymptotic value assumes the form

$$G_0 \sim 2(\omega/c)(1-\hat{r}^{-2})^{-\frac{1}{2}}\tilde{\zeta}^{\frac{1}{2}}(\tilde{\zeta}^3 - \tilde{\zeta}_b^3)^{-\frac{1}{2}}\cos[\tfrac{1}{3}\arcsin(\tilde{\zeta}_b/\tilde{\zeta})^{\frac{3}{2}}], \tag{64}$$

in which

$$\tilde{\zeta}_b^{\frac{3}{2}} \equiv 3(\tfrac{1}{2}\hat{r}\hat{r}_P)^{\frac{3}{2}}(1-\hat{r}^{-2})^{-\frac{3}{4}}\tilde{\phi}, \tag{65}$$

and $\hat{r}_P \gg 1$, $0 < \tilde{\zeta} \ll \hat{r}_P(\hat{r}^2-1)^{\frac{1}{2}}$, $|\tilde{\zeta}_b^{\frac{3}{2}}/\tilde{\zeta}^{\frac{3}{2}}| < 1$. Note that $\tilde{\zeta}_b^{\frac{3}{2}}$ denotes the value of $\tilde{\zeta}^{\frac{3}{2}}$ on the bifurcation surface, a value that is positive on the sheet $\phi = \phi_+$ and negative on the sheet $\phi = \phi_-$ of this surface (cf. (32), (56) and (62)). Moreover, it can be assumed without any loss of generality that the source distribution is localized about $z = 0$, and the colatitude of the observation point θ_P (see (61)) lies in the interval $(0, \frac{1}{2}\pi)$, so that $|\zeta| \equiv |\hat{z} - \hat{z}_P| = \hat{z}_P - \hat{z}$ by virtue of $\hat{R}_P \gg 1$ and hence

$$\tilde{\zeta} = \hat{z} - \hat{z}_P + \hat{r}_P(\hat{r}^2-1)^{\frac{1}{2}}. \tag{66}$$

Thus, at any given value of $\hat{r}$, the coordinates $\tilde{\zeta}$ and $\tilde{\phi}$ are related to $\hat{z}$ and $\hat{\varphi}$, respectively, by pure translations.

Let us further simplify the above expression for the Green's function G_0 by focusing attention on those source points that lie not only within the bifurcation surface close to its cusp curve but also in the neighbourhood of one of the sheets of this surface. For such source points, we also have $0 < 1 - |\tilde{\zeta}_b^{\frac{3}{2}}/\tilde{\zeta}^{\frac{3}{2}}| \ll 1$ and so we may replace $\tilde{\zeta}$ in (64) by $\tilde{\zeta}_b$, wherever possible, to obtain

$$G_0 \sim (\omega/c)(1-\hat{r}^{-2})^{-\frac{1}{2}}\tilde{\zeta}_b^{-\frac{1}{2}}(\tilde{\zeta} - \tilde{\zeta}_b)^{-\frac{1}{2}},$$
$$\hat{r}_P \gg 1, \quad 0 < \tilde{\zeta} \ll \hat{r}_P(\hat{r}^2-1)^{\frac{1}{2}}, \quad 0 < 1 - |\tilde{\zeta}_b^{\frac{3}{2}}/\tilde{\zeta}^{\frac{3}{2}}| \ll 1. \tag{67}$$

(The expression for G_0 is the same on both sheets of the bifurcation surface.)

To obtain the contribution of the source elements in question towards the value of the sound field, we must now insert the above expression for G_0 in (6) and perform the integration over the volume of the source. In order to be consistent, however, we should first approximate the source term $s(r, \hat{\varphi}, z)$ in (6) by its value in the immediate neighbourhood of the cusp curve of the bifurcation surface that is associated with an observation point in the far zone. On this locus, the variables $\hat{\varphi}$ and z in $s(r, \hat{\varphi}, z)$ can be eliminated with the aid of the parametric equation of the cusp curve ($\tilde{\phi} = 0$, $\tilde{\zeta} = 0$) to express the local value of the source density, $s|_{\tilde{\phi}=0, \tilde{\zeta}=0}$, as a function of $\hat{r}$ alone. The cusp curve associated with an observation point in the far zone lies almost entirely on a cylinder of radius $\hat{r} = \operatorname{cosec} \theta_P$ (see (75)), so that the interval in $\hat{r}$ over which this curve intersects a localized source distribution is of the order of $\hat{r}_P^{-1}$ only (according to (14), $\mathrm{d}\hat{r}/\mathrm{d}\hat{z} \approx \pm \hat{r}_P^{-1} \cos \theta_P$.) The difference between the exact value of the source density along the cusp curve and its average value

$$\langle s(r, \hat{\varphi}, z)|_{\tilde{\zeta}=0, \tilde{\phi}=0} \rangle \equiv \bar{s}_{cc} \tag{68}$$

over the r-interval in question, therefore, is negligibly small.

Once the G_0 given in (67) is inserted in (6), s is replaced with $\bar{s}_{cc}$ and (62) and (66) are used to change the variables of integration from $(r, \hat{\varphi}, z)$ to $(\hat{r}, \tilde{\phi}, \tilde{\zeta})$, the following expression results for the leading contribution to the sound generated by the source elements in the immediate vicinity of the cusp curve of the bifurcation surface:

$$\rho \sim (c/\omega)^2 \bar{s}_{cc} \int \mathrm{d}\hat{r}\, \mathrm{d}\tilde{\phi}\, \mathrm{d}\tilde{\zeta}\, \hat{r}(1-\hat{r}^{-2})^{-\frac{1}{2}} \tilde{\zeta}_b^{-\frac{1}{2}} (\tilde{\zeta} - \tilde{\zeta}_b)^{-\frac{1}{2}}. \tag{69}$$

The $\hat{z}$-quadrature in (6) over a short interval $\delta\hat{z} (\ll 1)$ right next to, and within, the bifurcation surface corresponds to an integration with respect to $\tilde{\zeta}$ in (69) from $\tilde{\zeta}_b$ to $\tilde{\zeta}_b + \delta\hat{z}$ (see (65) and (66)). Carrying out this integration, we obtain

$$\rho \sim (c/\omega)^2 \bar{s}_{cc} \int \mathrm{d}\hat{r}\, \mathrm{d}\tilde{\phi}\, \hat{r}(1-\hat{r}^{-2})^{-\frac{1}{2}} \int_1^{1+\delta\hat{z}/\tilde{\zeta}_b} \mathrm{d}\sigma (\sigma - 1)^{-\frac{1}{2}} \tag{70a}$$

$$\sim 2(c/\omega)^2 \bar{s}_{cc} (2\delta\hat{z})^{\frac{1}{2}} \hat{r}_P^{-\frac{1}{2}} \int \mathrm{d}\hat{r}\, \mathrm{d}\tilde{\phi}\, \hat{r}(\hat{r}^2 - 1)^{-\frac{1}{4}} (3\tilde{\phi})^{-\frac{1}{3}}, \tag{70b}$$

where use has been made of (65) to express $\tilde{\zeta}_b$ in terms of $\hat{r}$ and $\tilde{\phi}$. That the sound amplitude in the radiation zone decreases with the coordinate R_P of the observation point like $R_P^{-\frac{1}{2}}$, rather than R_P^{-1}, has now become evident since we shall see below that the value of the remaining integral in (70b) is independent of R_P.†

The way in which the non-spherical decay of the wave amplitude is brought about by the caustic can be seen from the structure of the definite integral on the right-hand side of (70a). According to (65), the range of this integral tends to zero like $\hat{r}_P^{-1}$ as $\hat{r}_P \to \infty$. Had its integrand been regular, therefore, the integral itself also would have decreased like $\hat{r}_P^{-1}$, and so the corresponding sound level would have decayed spherically. However, the singularity in the integrand of this integral – which reflects the presence of a bifurcation surface and hence a caustic – results in a value for the integral that tends to zero more slowly (like $\hat{r}_P^{-\frac{1}{2}}$) than its range does. That the decay rate is given by $\hat{r}_P^{-\frac{1}{2}}$ is clearly a consequence of the fact that the Green's function has an inverse square-root singularity, and this – as we shall see in §8 – is in turn related to the fact that the equation governing the present problem has the same structure as that governing (two-dimensional) axisymmetric waves in a non-homogeneous medium.

† Despite the appearance of $\operatorname{cosec}^{\frac{1}{2}} \theta_P$ in the factor $\hat{r}_P^{-\frac{1}{2}} = \hat{R}_P^{-\frac{1}{2}} \operatorname{cosec}^{\frac{1}{2}} \theta_P$ multiplying the integral in (70b), the right-hand side of this equation remains well behaved on the rotation axis: the quantity $s|_{\tilde{\zeta}=0, \tilde{\phi}=0}$, and hence $\bar{s}_{cc}$, vanishes for $\theta_P = 0$. According to (14), the cusp curve of the bifurcation surface associated with an observation point on the rotation axis crosses the plane $z = 0$ at too large a value of r to intersect a localized source.

The $\hat{\varphi}$-quadrature in (6) over a short interval $\delta\hat{\varphi}(\ll 1)$ next to the cusp curve of the bifurcation surface corresponds to an integration with respect to $\tilde{\phi}$ from zero to $\delta\hat{\varphi}$ in (72) (see (62) and (9)), and so results in

$$\rho \sim (c/\omega)^2 \bar{s}_{cc} (2\delta\hat{z})^{\frac{1}{2}} (3\delta\hat{\varphi})^{\frac{2}{3}} \hat{r}_P^{-\frac{1}{2}} \int \mathrm{d}\hat{r}\, \hat{r}(\hat{r}^2 - 1)^{-\frac{1}{4}}. \tag{71}$$

Since the cusp curve of the bifurcation surface lies almost entirely on the cylinder $\hat{r} = \operatorname{cosec}\theta_P$ when $\hat{r}_P \gg 1$ (see (75)), the source elements that contribute to the remaining integral in (71) lie within a short interval $\delta\hat{r}(\ll 1)$ next to $\hat{r} = \operatorname{cosec}\theta_P$. Thus in the case of an observation point with $\theta_P \neq \frac{1}{2}\pi$, for which the value of the integrand on this cylinder is both finite and non-zero, the integral is approximately given by the product of the value of the integrand at $\hat{r} = \operatorname{cosec}\theta_P$ with $\delta\hat{r}$:

$$\rho \sim (c/\omega)^2 \bar{s}_{cc} (2\delta\hat{z})^{\frac{1}{2}} (3\delta\hat{\varphi})^{\frac{2}{3}}\, \delta\hat{r} (\tfrac{1}{2}\sin 2\theta_P)^{-\frac{1}{2}} \hat{r}_P^{-\frac{1}{2}}, \quad \theta_P \neq \tfrac{1}{2}\pi. \tag{72}$$

However, in the case of an observation point in the plane of rotation $\theta_P = \frac{1}{2}\pi$, the cusp curve lies on the sonic cylinder $\hat{r} = 1$ at which the integrand in (71) is singular. Evaluating the improper integral in question over the interval $1 < \hat{r} < 1 + \delta\hat{r}$, we find that in this case

$$\rho \sim \tfrac{2}{3}(c/\omega)^2 \bar{s}_{cc} (2\delta\hat{z})^{\frac{1}{2}} (3\delta\hat{\varphi})^{\frac{2}{3}} (2\delta\hat{r})^{\frac{3}{4}} \hat{r}_P^{-\frac{1}{2}}, \quad \theta_P = \tfrac{1}{2}\pi, \tag{73}$$

in which we have ignored $\delta\hat{r}$ relative to unity. This expression differs from the limit of (72) for $\theta_P \to \frac{1}{2}\pi$; that is to say, the asymptotic expansion, of which (72) is the leading term, is not uniform with respect to the parameter θ_P.

Note that nowhere in the above derivation of (72) and (73) has it been necessary to specify the (spectral) distribution of the source density s as a function of $\hat{\varphi}$. The analysis in this section makes it clear that the cylindrical decay of the sound amplitude is a consequence solely of the behaviour of the Green's function G_0 on the cusp curve (14), i.e. of the radiation efficiency of the source elements that approach the observer with the wave speed and zero acceleration along the radiation direction, rather than of any specific properties of the steady source distribution in the blade-fixed frame. The conditions – on the spectral distribution of $s(r, \hat{\varphi}, z)$ as a function of $\hat{\varphi}$, and the distance of the observer relative to the Rayleigh distance – that were encountered when deriving the cylindrical decay of the sound amplitude in the frequency domain reflect limitations on the range of validity of the asymptotic technique used in §4 rather than on that of its result.

The limitation of the analysis in §4 stems from an inaccuracy of the high-frequency approximation in situations where the sources and the fields depend on one of the space coordinates and the time in a single combination only – as in the present case where the dependence of these quantities on φ and t only occurs in the combination $\hat{\varphi} = \varphi - \omega t$ (see also Appendix A). According to the time-domain analysis in this section, the main contribution towards the value of the sound field is made by the source elements for which both the argument $g(\varphi) - \phi$ of the delta function in (7) and its derivatives $\mathrm{d}g/\mathrm{d}\varphi$ and $\mathrm{d}^2g/\mathrm{d}\varphi^2$ vanish. These three conditions define the cusp curve of the bifurcation surface. According to the frequency-domain analysis, on the other hand, the leading contribution towards sound comes from the source elements for which the stationary points of the argument of the exponential function in (41) coalesce, i.e. for which $\mathrm{d}g/\mathrm{d}\varphi$ and $\mathrm{d}^2g/\mathrm{d}\varphi^2$ vanish. These two conditions on their own designate the projection of the cusp curve of the bifurcation surface onto the meridional plane $\hat{\varphi} = \text{const}$. That is to say, the asymptotic approximation that is used in §4 loses entirely the information contained in the structure of the caustic (cusp curve of the bifurcation surface) along the spatial dimension that is Fourier-analysed, and so treats the problem effectively as a two-dimensional one (see also §7). Had φ and t not appeared in a single combination, this limitation would not have arisen of course: in cases where the Fourier analysis is with respect to time alone, the projection affected by the high-frequency approximation is onto the hyperplane $t = \text{const.}$ and does not result in a loss of information about the structure of any caustics that may be present.

In fact, the concept of Rayleigh distance arises in the literature on wave theory in the specific context of diffraction by two-dimensional apertures (see e.g. Ziolkowski 1989). The Rayleigh criterion is a geometrical constraint – for the occurrence of constructive interference – on the distance of the observation point from the boundaries of a planar source distribution all of whose points radiate with the same efficiency. In the present problem, on the other hand, because the source elements that approach the observation point with the wave speed and zero acceleration radiate with a much greater efficiency in the direction of the observer than do any other source elements, the site of emission is a non-planar space curve which is determined by the position of the observation point itself and does not have a fixed shape or extent (§6). The shape of the locus of source elements that radiate most efficiently towards the given observation point is here such that these elements radiate in phase automatically, regardless of the value of the Rayleigh parameter.

6. Angular distribution of the radiation: compatibility of the results with the conservation of energy

The part of the cylindrically decaying radiation that contains the highest frequencies is detectable only in the orbital planes of the volume elements that constitute the source, i.e. over an interval in z_P that equals the z-extent, Δz, of the source distribution (§4). The energy associated with this part, therefore, is conserved manifestly: while the flux density of energy – which is proportional to ρ^2 – decreases like R_P^{-1} as we move away from the source, the area of a given cylindrical surface with the radius $\hat{r}_P = \text{const.} \gg 1$ and the height Δz, over which this part is detectable, increases like $2\pi r_P \Delta z$, so that the total flux of energy remains the same across all such cylindrical surfaces. But since the cylindrically decaying radiation is not exclusively confined to the orbital planes of the source elements, it seems at first sight that the flux of energy at an arbitrary frequency is not the same across spheres of different radii enclosing the source. This is not so, however. This apparent incompatibility with the conservation of energy is resolved once the beaming of the radiation is taken into account. Non-spherically decaying waves are quite different from most well-documented fields: they do not fill the space into which they propagate isotropically and they become more concentrated as they travel. Their decay must be as slow as their spreading to conserve energy, for the local strength of waves evolving into concentrated patches cannot exhibit the usual decay that is exhibited by isotropic waves.

The component of the radiation whose amplitude decays non-spherically is detectable only at those observation points in the far zone for which the cusp curve of the bifurcation surface intersects the source distribution (§5). The angular extent (in θ_P and $\hat{\varphi}_P$) of the radiation beam associated with this component, therefore, is determined by the shape of the curve described in (14) and by the distribution of the source density in the rotating frame. The projection of curve (14) onto the $(z,\hat{\varphi})$-plane, for an observation point that is located in the far zone, is given by

$$\hat{\varphi} - \hat{\varphi}_P \approx \hat{R}_P - \tfrac{1}{2}\pi - \hat{z}\cos\theta_P. \tag{74}$$

Moreover, if the source is assumed to be localized within a region containing $z = 0$, the second member of (14), which describes the projection of this cusp curve onto the (r, z)-plane, tends to

$$\hat{r} \approx \operatorname{cosec} \theta_P \tag{75}$$

in the limit where $\hat{r}_P \gg 1$ and $z_P \gg z$.

One implication of these relations is that the cusp curve of the bifurcation surface associated with an observation point in the far zone winds around a cylinder whose radius remains fixed over the extent of a localized source. Their second implication is that the latitudinal width of the radiation beam produced by a source distribution whose supersonic portion extends from $\hat{r} = 1$ to $\hat{r} = \hat{r}_0 > 1$ is given by the wide range of angles satisfying $\operatorname{cosec} \theta_P < \hat{r}_0$, i.e. by

$$\tfrac{1}{2}\pi - \arccos \hat{r}_0^{-1} < \theta_P < \tfrac{1}{2}\pi + \arccos \hat{r}_0^{-1}. \tag{76a}$$

This is because, for a value of θ_P outside the above range, the cusp curve of the bifurcation surface crosses the plane $z = 0$ at too large a value of r to intersect the source distribution: according to (14), the cusp curve in question touches the sonic cylinder $\hat{r} = 1$ at the single point $z = z_P, \phi = \phi_C$, and moves steadily away from it – by winding around cylinders of ever increasing radii – both for $z > z_P$ and $z < z_P$ (also see figure 4).

The longitudinal width $\Delta\hat{\varphi}_P$ of the radiation bean simply equals the longitudinal extent $\Delta\hat{\varphi}$ of the source distribution:

$$\Delta\hat{\varphi}_P = \Delta\hat{\varphi}, \tag{76b}$$

since a shift $\Delta\hat{\varphi}_P$ in the azimuthal position of any observation point results in an equal shift $\Delta\hat{\varphi}$ in the azimuthal position of the cusp curve associated with that observation point. According to (14), the cusp curves of the bifurcation surfaces belonging to two observation points with the coordinates $(r_P, \hat{\varphi}_P, z_P)$ and $(r_P, \hat{\varphi}_P + \Delta\hat{\varphi}_P, z_P)$ intersect a cylinder $\hat{r} = \text{const.} > 1$ at points whose z-coordinates are equal and whose $\hat{\varphi}$-coordinates differ by $\Delta\hat{\varphi} = \Delta\hat{\varphi}_P$. The non-spherically diverging signals that are detected at $(r_P, \hat{\varphi}_P, z_P)$ and $(r_P, \hat{\varphi}_P + \Delta\hat{\varphi}_P, z_P)$, therefore, receive contributions from those source points on a circle $\hat{r} = \text{const.} > 1$, $z = \text{const.}$, which are apart by the angle $\Delta\hat{\varphi} = \Delta\hat{\varphi}_P$. Hence, when the points on the circle mark the boundaries of a localized source, the width of the overall waveform equals $\Delta\hat{\varphi}$.

Before addressing the issue of how an emission into such a wide solid angle as (76) is compatible with the conservation of energy, we must also consider the mapping between an interval Δt of (retarded) emission time and the corresponding interval Δt_P of observation time. All source points on the bifurcation surface approach the observation point with a velocity whose component along the radiation direction equals the speed of sound; the source points on the cusp curve of the bifurcation surface in addition approach the observer with zero acceleration along this direction (see Ardavan 1991 *a*). For the source points that give rise to the cylindrically decaying radiation, therefore, a finite interval of (retarded) emission time is Doppler shifted to a vanishing interval of observation time. Given a rotating source point with the fixed coordinates $(r, \hat{\varphi}, z)$ and a stationary observation point with the fixed coordinates (r_P, φ_P, z_P), it follows from $\mathrm{d}\hat{\varphi} = \mathrm{d}\varphi - \omega \mathrm{d}t = 0$ and $\mathrm{d}\varphi_P = \mathrm{d}\hat{\varphi}_P + \omega \mathrm{d}t_P = 0$ that the ratio $\mathrm{d}t_P/\mathrm{d}t$ of the observation to the emission time intervals has the value $-\mathrm{d}\hat{\varphi}_P/\mathrm{d}\varphi$ which, according to (9), equals $\mathrm{d}g/\mathrm{d}\varphi$. The bifurcation surface and its cusp curve, on the other hand, are by definition the loci of the points at which $\mathrm{d}g/\mathrm{d}\varphi = 0$ and $\mathrm{d}^2g/\mathrm{d}\varphi^2 = 0$, so that for such points $\mathrm{d}t_P/\mathrm{d}t = 0$.

For those volume elements of an extended source that do not lie right on the bifurcation surface, the emitted wave fronts do not crowd together to such an extent that the ratio of the observation to the emission time intervals vanishes exactly. Nonetheless, the Doppler factor $dg/d\varphi$ appearing in (8) ensures that the ratio in question – which depends on R_P – has exceedingly small values for the filamentary part of the source at the cusp curve of the bifurcation surface that radiates coherently and so gives rise to the non-spherically decaying signal. The inverse square-root singularity of the leading term in the asymptotic expansion (67) of the Green's function at its caustic – which arises from the vanishing of the Doppler factor $dg/d\varphi$ in (8) – shows that for the source points neighbouring the cusp curve the ratio of the observation to the emission time intervals approaches zero like the square root of the distance $\tilde{\zeta}-\tilde{\zeta}_b$ from the bifurcation surface. When we integrate the Green's function over a neighbourhood of the cusp curve (in (69)), we find that the contribution arising from the singularity introduces an extra factor of $R_P^{\frac{1}{2}}$ into expression (70) for the sound strength that would have been absent had the Doppler factor been non-vanishing. The effective value of the ratio dt_P/dt for the source points that lie in the neighbourhood of the cusp curve, therefore, is smaller the larger R_P is.

Since in the present case the sound field depends on φ_P and t_P in the combination $\varphi_P-\omega t_P$ only, the smallness of the ratio dt_P/dt for the source points in the neighbourhood of the singularity of the Green's function translates into the narrowness of the azimuthal width of the subpulse that is produced by the filamentary locus of volume elements at the intersection of the cusp curve of the bifurcation surface with the source distribution. The fact that dt_P/dt is smaller the larger R_P is implies that the longitudinal widths of the subpulses in question are narrower the further away we move from the source. The requirements of the conservation of energy are met in the case of the signal produced by an individual filament, therefore, because the fact that ρ^2 should be decreasing like R_P^{-1}, rather than like R_P^{-2}, is demanded by the reduction in the longitudinal width of such a signal with range. In other words, the enhancement of the flux density of energy at the position of the observer is compensated by a corresponding reduction in the size of the area subtended by the radiation beam of the filament. (Note, however, that, over essentially all of the solid angle covering the region outside a given subpulse, the emission from the filamentary source of that subpulse decays spherically.) If it were possible to move the observation point away from the source in such a way that the cusp curve of the bifurcation surface intersected the source distribution along the same segment at all R_P, then the fact that the retarded potential (3) – from which (72) was derived – is both consistent with the conservation of energy and automatically contains the Doppler factor $dg/d\varphi$ (see (8)) would have implied that the width of the signal would decrease with increasing R_P like R_P^{-1}. In general, however, no two subpulses within the waveforms that are observed at different distances have identical filaments as their sources, so that the R_P-dependence of the width of an individual subpulse is not well defined.

Insofar as a cylindrically diverging subpulse can be detected at any observation point that lies within the solid angle (76), the overall radiation beam consists of a superposition of the narrow beams that are produced by the filamentary sources described above. The filamentary sources also generate a sound field which decays spherically outside the narrow radiation beams in question. However, as far as the cylindrically decaying component of the radiation is concerned, the different subpulses constituting the waveform are each generated by a different filamentary part of the source. Since the signals received at two neighbouring points of region (76) on a sphere $\hat{R}_P = \text{const.} \gg 1$ arise from filaments that have both different extents and different strengths, the resulting overall waveform thus consists of the superposition of a (continuous) set of 'spiky' subpulses with uneven and fluctuating amplitudes.

The energy associated with the overall waveform is conserved because that associated with each individual subpulse is. That the radiation beam (76) spreads spherically, while the flux density of the energy radiated by each filament – and associated with each subpulse – decays non-spherically, is not incompatible with the requirements of the conservation of energy because the distribution of the intensity of the radiation across the beam is not independent of R_P. Just as the radiation received at different points on $R_P = \text{const.}$ is generated by different filamentary parts of the source, so also the emissions received at the same $(\theta_P, \hat{\varphi}_P)$ but different values of R_P arise from different source elements: any change in the position of the observation point changes the segment along which the cusp curve of the bifurcation surface intersects the source distribution. The site of emission of each subpulse is determined by the position of the observation point itself, and it is not possible to identify a unique source distribution for the different waveforms that are observed at different distances. The subpulse structure associated with the variations in the intensity of the radiation with angles θ_P and $\hat{\varphi}_P$, therefore, has a pattern that changes radically as the distance R_P changes. This change, in conjunction with the fact that the subpulses are narrower the further away we move from the source, explains how the *average* value of the flux density ρ^2 over the surface of the sphere $R_P = \text{const.}$ will – in compliance with the conservation of energy – decay like R_P^{-2}, while at the same time the flux density of energy associated with an individual subpulse would differ from its near-field value by the factor R_P^{-1}.

Although being generally unfamiliar, the above features are also exhibited by the radiation emitted by simple model systems. Imagine, for instance, a set of point sources, randomly located on the circumference of a circle of radius L, which are initially at rest and which simultaneously move in straight lines at the supersonic speed u, with zero acceleration, to the points diametrically opposite their original positions and abruptly come to rest once again. An observer detecting the resulting radiation in the far zone would receive a pulse with the width $2L/u$ if her line of sight does not make the angle arccos (c/u) with the trajectory of any of the point sources; otherwise, she would in addition receive an impulsive signal as she is hit by the Mach wave of one of the sources. The additional large-amplitude component of the radiation is generated by the crowding together of the wave fronts that emanated from a single one of the point sources as it moved to its new position, i.e. from a limited part of the source distribution. This component of the radiation does not decay spherically but, by virtue of being observable only during a time interval that is vanishingly smaller than the emission time $2L/u$, carries the same amount of energy across all spheres that enclose the source.

For a more realistic example of a system illustrating these features, and a demonstration of the fact that the retarded potential takes account of the conservation of wave energy automatically, see Ffowcs Williams & Guo (1988) and Guo (1990). See also the examples of propagating wavepackets known as acoustic or electromagnetic 'missiles' given by Myers *et al.* (1990), and the references therein, and by Ffowcs Williams (1993*a*, *b*). The non-spherically decaying wave packets – or 'missiles' – of diminishing duration discussed in these references are basically no different from the individual subpulses encountered in the present paper; except that, here, the volume distribution of quadrupole sources, by acting as a continuous collection of continually operating 'missile' launchers each of which points in a different direction, gives rise to an emission of this type that propagates over a *wide* solid angle. (That the particular examples of the acoustic and electromagnetic missiles so far described in the literature decay non-spherically only within a certain Rayleigh distance is a consequence of the fact that they are invariably generated by finite-extent *planar* source distributions (cf. Ziolkowski 1989).)

7. Comparison of the results with those of earlier works

A basic feature of published treatments of the steady rotating-blade noise problem is that they are all based – in most cases implicitly – on various asymptotic properties of the Green's function that appears in (17). The exact expression for the mth Fourier component of this Green's function is

$$\hat{G}_{0m} = \mathrm{i}(\omega/c)\int_0^\infty J_m(\lambda\hat{r}_<)\,H_m^{(1)}(\lambda\hat{r}_>)\cos[k(\hat{z}-\hat{z}_P)]\,\mathrm{d}k, \tag{77}$$

where

$$\lambda \equiv \begin{cases} m(1-k^2/m^2)^{\frac{1}{2}}, & k^2 < m^2, \\ \mathrm{i}(k^2-m^2)^{\frac{1}{2}}, & k^2 > m^2, \end{cases} \tag{78}$$

with real and positive square roots. Here, $\hat{r}_<(\hat{r}_>)$ is the smaller (larger) of $\hat{r}_P$ and $\hat{r}$, J_m is the Bessel function of order m and $H_m^{(1)}$ is the Hankel function of the first kind and mth order. (For the derivation of this expression see Hanson 1983, Tam 1983, and Ardavan 1984.)

To obtain the far-field approximation to $\hat{G}_{0m}$, the Hankel function in (77) is replaced by its asymptotic value for large argument ($\hat{r}_P \gg 1$) and real λ,

$$H_m^{(1)}(\lambda\hat{r}_P) \sim (\tfrac{1}{2}\pi\lambda\hat{r}_P)^{-\frac{1}{2}}\exp[\mathrm{i}(\lambda\hat{r}_P-\tfrac{1}{2}m\pi-\tfrac{1}{4}\pi)], \quad m>0, \tag{79}$$

which dominates the corresponding value of this function for imaginary λ (cf. formulae (9.2.3) and (9.7.2) of Abramowitz & Stegun 1970). Then the evaluation of the resulting integral over k by the method of stationary phase yields

$$\hat{G}_{0m} \sim (\omega/c)\,\hat{R}_P^{-1}\exp[\mathrm{i}m(\hat{R}_P-\hat{z}\cos\theta_P-\tfrac{1}{2}\pi)]\,J_m(m\hat{r}\sin\theta_P), \quad m>0. \tag{80}$$

This is the expression, derived by Hawkings & Lowson (1974), Hanson (1980), Ardavan (1981), and Tam (1983), whose generalization to the case of a helically moving source has been adopted as the point of departure for several recent studies of high-speed propeller noise (see e.g. Parry & Crighton 1989; Crighton & Parry 1991; Peake & Crighton 1991*a*, *b*). It states that the sound amplitude decays spherically, and – as the kernel in the radiation integral (15) – it implies that the main contribution towards the value of ρ_m for $m \gg 1$ is made by the source elements at the cylindrical surface $\hat{r} = \operatorname{cosec}\theta_P$, where the argument of the Bessel function $J_m(m\hat{r}\sin\theta_P)$ equals its order. Crighton & Parry (1991) and Peake & Crighton (1991*a*, *b*) refer to $\hat{r} = \operatorname{cosec}\theta_P$ as the Mach radius; Ardavan (1981) emphasized the equivalent cylinder as the likely site of emission for the electromagnetic radiation received from pulsars.

We have seen (§3) that the locus at which G_0 attains its sharpest singularity is the cusp curve of the bifurcation surface, and that this curve, for an observation point that is located in the far zone and a source distribution that is localized about $z=0$, lies on, and winds around, the cylindrical surface $\hat{r} = \operatorname{cosec}\theta_P$ (cf. (75)). Thus, the far-field and high-frequency approximations replace the locus where the radiation efficiency peaks by a surface containing this curve. (The high-frequency approximation, on its own, replaces this curve with the surface of rotation generated by its projection onto the meridional plane $\hat{\varphi} = \text{const.}$ (see §5).) The conclusion reached in Ardavan (1981), and in Peake & Crighton (1991*a*), that in the limit of high frequencies the emission received at the colatitude θ_P in the far zone arises from the source elements at the intersection of the Mach cylinder with the volume of the source is not exact. The crucial point at which new ground is broken in the present analysis is that where the loci of singularities of the Green's function G_0 have been treated exactly. It is the error in the usually good approximations on which the conclusion by Ardavan (1981) and Peake & Crighton (1991 *a*) is based that gives rise to the non-spherically diverging pulses identified in this paper, pulses whose formation by the constructive interference of the contributions from differenct source points on the cusp curve depends crucially on the deviations of this curve from its approximating surface. The consequences of the fact that it is the cusp curve of the bifurcation surface that delineates the site of emission, and not the cylinder $\hat{r} = \operatorname{cosec}\theta_P$, are potentially great because they lead to pulses that decay more slowly and therefore are bigger than spherically spreading waves in the far zone.

Neither the surfaces of the rotor blades nor the shock discontinuities attached to them (cf. Hanson & Fink 1979; Farassat & Myers 1989; Peake & Crighton 1991 *a, b*) could in general fall within the site of this enhanced emission: the cusp curve of the bifurcation surface could at best intersect any discontinuities in the near-field flow at a few isolated points. Our cylindrically decaying radiation that could dominate the distant sound would arise from the coherent emission of the source elements along the cusp curve and should be insensitive to the presence or absence of a few such isolated source points.

A further limitation of the usual far-field approximation, which is actually more serious than its misplacing the site of emission, is that by altering the structure of the phase of the exponential function in the integrand of (17), it misses out the non-spherically decaying component of the radiation altogether. The far-field expression (80) is what follows from (17) when the phase function $g(\varphi) = \varphi-\varphi_P-\omega|\boldsymbol{x}-\boldsymbol{x}_P|/c$ (see (9)) is approximated by the first two terms in its Taylor expansion in powers of $|\boldsymbol{x}|/|\boldsymbol{x}_P|$. Unless some of the higher-order terms in this Taylor expansion are also retained, the resulting expression would not be an exact enough representation of $g(\varphi)$ for the effects arising from the source elements at the locus of coalescence of the critical points of this function to show up. To extract the non-spherical decay terms, it is essential that $g(\varphi)$ is transformed into, or at least approximated by, a cubic function of φ, as in §3, and that the coefficients in this cubic function are only approximated by expressions that remain uniformly valid at any source point on the cusp curve of the bifurcation surface and at all observation points – as in §5.

The high-frequency approximation to $\hat{G}_{0m}$ may be obtained by noting that the product of the Bessel functions in (77) is exponentially small when $|k|$ is of the order of or greater than $|m|$ (cf. formulae (9.3.2), (9.7.7) and (9.7.8) of Abramowitz & Stegun 1970). We may therefore replace λ with its value for $k^2 \ll m^2$, i.e. m, take the resulting Bessel functions outside the integral sign, and perform the simple integration that remains to arrive at

$$\hat{G}_{0m} \sim \mathrm{i}\pi(\omega/c)\, J_m(m\hat{r}_<)\, H_m^{(1)}(m\hat{r}_>)\, \delta(\hat{z}-\hat{z}_P), \quad m \to \infty \tag{81}$$

(see Ardavan 1989). The final result of §4, equation (48), can in fact be obtained from this expression directly. If (81), with $\hat{r}_> = \hat{r}_P$ and $\hat{r}_< = \hat{r}$, is inserted in the expression for ρ_m defined by (15) and (40), and the trivial integration over $\hat{z}$ is performed, then the integrand of the remaining integral over $\hat{r}$ turns out to be the same as that of the Hankel transform of $s_m|_{\zeta=0}$. The kernel $J_m(m\hat{r})$ of the Hankel transform in question, on the other hand, is in the asymptotic regime $m \to \infty$ expressible in terms of an Airy function whose peak occurs at $\hat{r} = 1$. So, we may approximate $s_m|_{\zeta=0}$ in the integral over $\hat{r}$ by $s_m|_{\zeta=0,\hat{r}=1}$ and extend the range of integration to the interval $(0, \infty)$. Once the resulting integral is evaluated (by formula (11.4.17) of Abramowitz & Stegun 1970), and $H_m^{(1)}(m\hat{r}_P)$ is replaced with the leading term in its asymptotic expansion for large m (by formula (9.3.3) of Abramowitz & Stegun 1970), we obtain an expression for ρ_m that is precisely the same as that given in (48). From (81), it also follows that in contrast to the radiation generated by a subsonic source distribution, whose spectrum has an exponential cut-off at high frequencies, the spectrum of the present emission has a power-law decay throughout the range of frequencies $m \gg 1$ in which the Fourier transform of the source density is non-zero.

Since the amplitude of $H_m^{(1)}(m\hat{r}_P)$ decays like $\hat{r}_P^{-\frac{1}{2}}$ for $\hat{r}_P \to \infty$ (see (79)), the far-field approximation to expression (81) is not the same as the high-frequency limit of (80). Obviously, it makes a difference whether we first calculate $\hat{G}_{0m}$ for $R_P \to \infty$ and then let $m \to \infty$ (in which case the sound amplitude decays spherically), or whether we first calculate $\hat{G}_{0m}$ for $m \to \infty$ and then let $R_P \to \infty$ (in which case the sound amplitude decays cylindrically). The far-field approximation alters the structure of the phase function g that appears in (17) so radically as to obliterate the more slowly decaying contribution altogether.

Since the asymptotic expressions derived in this paper cannot be directly differentiated, a technical point concerning the calculation of the gradient of the sound amplitude needs to be mentioned. To differentiate the exact expression (15) under the integral sign, we must exclude the bifurcation surface from the domain of integration to begin with, and only proceed to the limit in which the volume of the excluded region shrinks to zero after having completed the calculation. This procedure results in two different contributions towards the value of the radial gradient $\partial\rho/\partial r_P$: a surface integral arising from the boundaries of the excluded region (which happens to survive in the limit in which the volume of the excluded region vanishes), and a volume integral involving the derivative of the integrand. The leading term in the asymptotic expansion of the contribution from the boundaries of the excluded region is beamed into the plane of rotation and behaves like $\hat{r}_P^{-\frac{1}{2}} m^{-\frac{5}{6}}$ for $m \gg 1$ and $\hat{r}_P \gg 1$ (see equation (31) of Ardavan 1991*b*). However, an asymptotic analysis of the contribution involving the derivative of the integrand, by the method presented in §4, shows that the leading term in the expansion of this latter contribution behaves like $\hat{r}_P^{-\frac{1}{2}} m^{-\frac{1}{2}}$ in the same regime (see Appendix B). So, although responsible for the breakdown of the linearized theory in the near zone (Ardavan 1991*a*, *b*), the contribution from the boundaries of the excluded region may be ignored as far as the high-frequency radiation in the far zone is concerned.

8. Concluding remarks

In so far as the only assumption we have made in the present paper concerning the source distribution is that it is steady in the rotating frame (see (4)), our analysis applies to the monopole and dipole as well as the quadrupole term in the Ffowcs Williams–Hawkings equation. However, from the fact that the non-spherically decaying component of the radiation arises from the source elements at the intersection of the cusp curve of the bifurcation surface with the source distribution, it follows that the signal observed in the far zone is generated by the quadrupole sources alone. Since the distributions of the monopole and dipole sources are two-dimensional, the cusp curve of the bifurcation surface can only intersect them at two isolated points on the upper and lower surfaces of the rotor blade. Only the elements belonging to the quadrupole sources that are distributed over a volume can possibly lie on an extended segment of this cusp curve and so contribute towards a strong component of the sound field.† We conclude with the suggestion that the radiation efficiencies of the volume source elements which approach the observer with the speed of sound and zero acceleration along the radiation direction are – when they occur – likely to exceed those of any other source elements by the large factor $\hat{R}_P^{\frac{1}{2}}$.

That the enhanced efficiency of these source points should result in the factor $\hat{R}_P^{\frac{1}{2}}$, rather than $\hat{R}_P^{\alpha}$ with a different value of α, may be inferred directly from the mathematical structure of the governing equation for the present problem. The ordinary wave equation (1) under the assumption that the sound and its sources are steady in the rotating frame, i.e. subject to symmetry (4), reduces to

$$\frac{1}{r}\frac{\partial}{\partial r}\left(r\frac{\partial \rho}{\partial r}\right)+\frac{\partial^2 \rho}{\partial z^2}+\left(\frac{1}{r^2}-\frac{\omega^2}{c^2}\right)\frac{\partial^2 \rho}{\partial \hat{\varphi}^2}=-4\pi s(r,\hat{\varphi},z), \tag{82}$$

which is an equation of the mixed type: it is elliptic in $r < c/\omega$ and hyperbolic in $r > c/\omega$. What in the four-dimensional (r,φ,z,t)-space appears as the bifurcation surface is from the point of view of the lower-dimensional $(r,\hat{\varphi},z)$-space the ray conoid of (82) in its domain of hyperbolicity (see Ardavan 1989, §6). From this latter point of view, we can regard the variable $\hat{\varphi}/\omega$ in the domain $r > c/\omega$ as a time coordinate and interpret (82) as the wave equation governing the generation and propagation of axisymmetric waves in a non-homogeneous medium for which the speed of sound varies like $[1-c^2/(r\omega)^2]^{-\frac{1}{2}}c$ with the distance r from the axis of symmetry. Then the fact that the Green's function for (82) should have an inverse square-root singularity, or that the waves propagating along a caustic of the ray conoid (the cusp curve of the bifurcation surface) should decay cylindrically, become mathematical consequences of the reduction in the dimension of the wave equation (see Courant & Hilbert 1962).

The filamentary part of the source which moves towards the observer at the wave speed with its normal parallel to the radiation direction, and so acts as the site of emission, owes its organized and extended structure to the fact that the flow in the blade-fixed frame is steady. For there to be a dense set of source points that radiate coherently, this symmetry of the flow which underlies the structure of the bifurcation surface described in §2 is essential: the focusing of the rays from a few isolated source points is not sufficient for generating a non-spherically decaying signal. It follows, therefore, that the noise in the far zone should be suppressed by any effect that breaks this symmetry of the flow, i.e. that renders the quadrupole sources in the region surrounding the blade unsteady as viewed from the rotating frame. (See also Ardavan 1991*a*.)

We have identified a slowly decaying component of propeller noise, a previously unidentified element but the element with the largest far-field amplitude, which is predominantly beamed into the plane of rotation (§5), and is composed of a continuous collection of 'spiky' subpulses with highly uneven amplitudes (§6). This might well be responsible for the acute sensation of crackling which has been experimentally known since the early works of Bryan (1920) and Hilton (1939). The new element has a surprisingly slow rate of decay and enters only a specific, but extensive, region of space: its amplitude decays like $R_P^{-\frac{1}{2}}$ at those colatitudes, on both

† For blade surfaces whose shapes are sufficiently close to the shape of one of the sheets of the bifurcation surface in the vicinity of the point $C(\hat{r}=1,\, z=z_P,\, \phi=\phi_C)$, the sound amplitude arising from the monopole and dipole sources can decay non-spherically (Ffowcs Williams & Hawkings 1969, p. 340), or even diverge at the associated observation point (Ardavan 1991*a*, p. 662). However, this type of non-spherical decay – which is caused by the source elements whose space-time trajectories have highly degenerate points of tangency with the past light cone of the observer – can only occur under special circumstances and must accordingly be regarded as a special case of the generic phenomenon discussed here.

sides of the plane of rotation, that satisfy $\operatorname{cosec}\theta_P < r_0\omega/c$. This component is in addition to the conventionally studied component of the propeller noise which decays like R_P^{-1} – but is likely to dominate it at large range. There seem to be no experimental data available on these far-field decay rates in the published literature on the subject; the existing data are all concerned with the decay of the sound amplitude in the near field, from which little can be learnt that bears on the distant sound.

We have in this paper derived the wave characteristics by means of an analysis in the time domain (§5), so that although the more slowly decaying component of the radiation is also that which contains the higher harmonics of the rotation frequency (§4), the decay rate in question is not confined to these higher frequencies. The cylindrically decaying component of the radiation contains the lower as well as the higher harmonics of the rotation frequency and might well propagate into the far field regardless of the fact that high-frequency acoustic waves are subject to atmospheric attenuation. To what extent effects associated with nonlinear wave propagation – such as those that enter the formation of sonic booms – would influence this component of the radiation is of course a question that remains open, though it is not one that is difficult to address in the light of the techniques already developed by Whitham (1974) and Lighthill (1993).

I am indebted to J. E. Ffowcs Williams for illuminating discussions and for his reading the manuscript and making comments and suggestions that improved it. I am also grateful to F. Farassat for drawing my attention to Myers & Farassat (1987), to D. Lynden-Bell for helpful conversations, and to A. M. Cargill, D. G. Crighton, A. P. Dowling, N. Peake and P. R. Prentice for stimulating comments and criticisms.

Appendix A. The radiation by finite-duration rectilinearly moving supersonic sources

The radiation that is discussed in the text has many features in common with that emitted by a source of the same type which moves with a supersonic speed along a rectilinear path. Although most aspects of the radiation arising from a rectilinearly moving source are known (see e.g. Whitham 1974; Dowling & Ffowcs Williams 1983), the properties of this radiation in the case where the source is of finite duration do not seem to have been discussed in detail before. Here we include an analysis of these properties, in both the time and the frequency domains, to emphasize the following two points: (i) that cylindrically decaying pulses arise also when a rectilinearly moving volume source of *arbitrarily short duration* approaches the observer – along the radiation direction – with the wave speed and zero acceleration at the retarded time, and (ii) that the limitation of the frequency-domain analysis, which gives rise to a spurious constraint on the Rayleigh parameter (cf. §4), also shows up in the present context. Inasmuch as the circular trajectories of the volume elements constituting a rotating source can be locally approximated by short-duration rectilinear trajectories, the results discussed in this appendix may be regarded as the preliminary versions of those reported in §§5 and 6 of the text.

Suppose that an extended source, that is steady in its own rest frame, moves with a constant supersonic speed, $u > c$, along the z-axis of a Cartesian coordinate system (x, y, z) and has the finite duration $0 < t < T$; the density for such a source has the form

$$s(x, y, z, t) = s(x, y, \hat{z})\,[\theta(t) - \theta(t-T)], \tag{A 1}$$

where

$$\hat{z} \equiv z - ut, \tag{A 2}$$

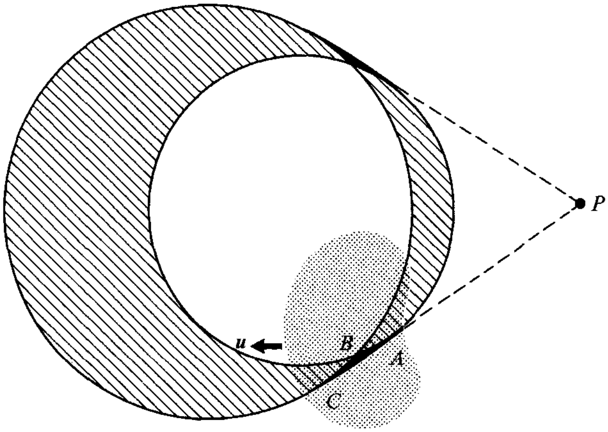

FIGURE 5. The domain of dependence of the observation point P for a finite-duration source (occupying the dotted space) which moves rectilinearly with the supersonic velocity $\boldsymbol{u}$. The boundary of the domain consists of a section of the inverted Mach cone issuing from P and portions of two spheres that are tangent to this cone. Region I of this domain, which is here shown in black, lies within the cone but outside the two spheres, and region II, which is hatched, comprises the union of the two spheres less their intersection.

and θ is the Heaviside step function. When we insert (A 1) in the retarded solution (3) of the wave equation (1) and change the variables (x, y, z, t) to $(x, y, \hat{z}, t)$, we find that the sound generated by such a source is described by

$$\rho(x_P, y_P, \hat{z}_P, t_P) = \int \mathrm{d}x\,\mathrm{d}y\,\mathrm{d}\hat{z}\, s(x, y, \hat{z})\, G_1, \tag{A 3}$$

in which the Green's function G_1 is defined by

$$G_1 \equiv \int_0^T \mathrm{d}t\, \delta(t_P - t - R/c)/R, \tag{A 4}$$

with $\hat{z}_P \equiv z_P - ut_P$, and

$$R \equiv \{(x-x_P)^2 + (y-y_P)^2 + [\hat{z} - \hat{z}_P + u(t-t_P)]^2\}^{\frac{1}{2}}. \tag{A 5}$$

The integral in (A 3) extends over all values of $(x, y, \hat{z})$ for which the source density s is non-zero.

Not unexpectedly, the Green's function appearing in (A 3) differs only slightly from that encountered in the standard analysis of Mach radiation. Evaluation of the integral in (A 4) yields

$$G_1 = \frac{\theta[\hat{z} - \hat{z}_P - (M^2-1)^{\frac{1}{2}} R_\perp]}{[(\hat{z}-\hat{z}_P)^2 - (M^2-1)\, R_\perp^2]^{\frac{1}{2}}}[\theta(t_+) + \theta(t_-) - \theta(t_+ - T) - \theta(t_- - T)], \tag{A 6}$$

where

$$t_\pm = t_P - c^{-1}(M^2-1)^{-1}\{M(\hat{z}-\hat{z}_P) \pm [(\hat{z}-\hat{z}_P)^2 - (M^2-1)\, R_\perp^2]^{\frac{1}{2}}\}, \tag{A 7}$$

$$R_\perp \equiv [(x-x_P)^2 + (y-y_P)^2]^{\frac{1}{2}}, \tag{A 8}$$

and $M \equiv u/c$. The combination of the step functions involving $t_\pm$ in (A 6) arise from the finiteness of the duration of the source.

For any given observation point $(x_P, y_P, \hat{z}_P)$, the Green's function G_1 is non-zero only inside a region of $(x, y, \hat{z})$-space, shown in figure 5, that is bounded by the inverted Mach cone

$$\hat{z} - \hat{z}_P = (M^2-1)^{\frac{1}{2}} R_\perp \tag{A 9}$$

and the following two spheres:

$$(\hat{z}-\hat{z}_P-ut_P)^2+R_\perp^2 = c^2t_P^2, \tag{A 10}$$

$$[\hat{z}-\hat{z}_P-u(t_P-T)]^2+R_\perp^2 = c^2(t_P-T)^2. \tag{A 11}$$

Within this domain of dependence of the observation point, we have

$$G_1 = [(\hat{z}-\hat{z}_P)^2-(M^2-1)\,R_\perp^2]^{-\frac{1}{2}}\begin{cases}1 & \text{in region I,}\\ 2 & \text{in region II,}\end{cases} \tag{A 12}$$

where region I lies inside the cone but outside the two spheres, and region II consists of the union of the two spheres less their intersection (see figure 5). The factor of 2 by which the value of G_1 changes from one region to the other reflects the number of waves that are simultaneously received at P from the source points in these regions.

Let us now consider a far-field observation point, P, for which the inverted Mach cone (A 9) intersects the source distribution, and calculate the contribution towards the sound at P from those volume elements of the source that lie in the following neighbourhood, N, of this cone:

$$R_{\perp A} \leqslant R_\perp \leqslant R_{\perp C}, \tag{A 13}$$

$$(M^2-1)^{\frac{1}{2}}R_\perp \leqslant \hat{z}-\hat{z}_P \leqslant \begin{cases}Mct_P-(c^2t_P^2-R_\perp^2)^{\frac{1}{2}}, & R_{\perp A} < R_\perp < R_{\perp B}\\ Mct'_P-(c^2t'^2_P-R_\perp^2)^{\frac{1}{2}}, & R_{\perp B} < R_\perp < R_{\perp C},\end{cases} \tag{A 14}$$

$$\varphi_< \leqslant \varphi \leqslant \varphi_>, \tag{A 15}$$

where

$$t'_P \equiv t_P-T, \tag{A 16}$$

$$\begin{bmatrix}R_{\perp A}\\ R_{\perp B}\\ R_{\perp C}\end{bmatrix} \equiv (1-M^{-2})^{\frac{1}{2}}c\begin{bmatrix}t'_P\\ [t_P t'_P-\frac{1}{4}(M^2-1)\,T^2]^{\frac{1}{2}}\\ t_P\end{bmatrix} \tag{A 17}$$

denote the values of $R_\perp$ for the points A, B, C shown in figure 5, and the bounds on the azimuthal angle $\varphi \equiv \arctan(y/x)$ satisfy the constraints

$$\varphi_> = \varphi_P+\arcsin[(1-M^{-2})^{\frac{1}{2}}r_P^{-1}\,ct'_P], \tag{A 18}$$

$$\varphi_>-\varphi_< \leqslant 2\pi. \tag{A 19}$$

The space-time coordinates $r_P \equiv (x_P^2+y_P^2)^{\frac{1}{2}}$ and t_P of the observation point are here assumed to be such that the argument of the inverse trigonometric function in (A 18) is less than or equal to unity. That is to say, the observation point is assumed to be located within a corresponding neighbourhood of the truncated Mach cones in the $(r_P, \varphi_P, \hat{z}_P)$-space which issue from the source distribution (cf. the limiting form of (A 17) for $r \equiv (x^2+y^2)^{\frac{1}{2}} \ll r_P$)

Neighbourhood N has an extension of the order of cT in r and a thickness of the order of cT^2/t_P in $\hat{z}$; it, therefore, has a vanishing volume in the limit $t_P \rightarrow \infty$ and so is entirely contained within the source distribution when this distribution has a lengthscale larger than cT. In order that we may approximate the source density s by its average value $\bar{s}$ within N, here we shall only consider a value of cT that is much smaller than the lengthscale of variation of the source density.

Once we replace s in (A 3) by the constant $\bar{s}$, the integral of G_1 over neighbourhood N can in fact be evaluated exactly. The integration with respect to $\hat{z}$ over the interval (A 14) yields

$$\int G_1\,\mathrm{d}\hat{z} = \operatorname{arccosh}\chi-\operatorname{arctanh}M^{-1}+t_P \rightarrow t'_P, \tag{A 20}$$

where
$$\chi \equiv ct_P/R_\perp, \tag{A 21}$$
and $t_P \to t'_P$ stands for two terms like the ones preceding it in which t_P is everywhere replaced with t'_P. The remaining integrals, after a change of variables from (x, y) to $(R_\perp, \varphi)$, can be written as

$$\int_N G_1 \,\mathrm{d}x\,\mathrm{d}y\,\mathrm{d}\hat{z} = \int_{\varphi_<}^{\varphi_>} \mathrm{d}\varphi \int_{R_{\perp A}}^{R_{\perp C}} \mathrm{d}R_\perp\, R_\perp \left\{1 - \frac{r_P \cos(\varphi - \varphi_P)}{[R_\perp^2 - r_P^2 \sin^2(\varphi-\varphi_P)]^{\frac{1}{2}}}\right\}$$
$$\times(\operatorname{arccosh}\chi - \operatorname{arctanh} M^{-1}) - t_P \leftrightarrow t'_P, \tag{A 22}$$

where (r_P, φ_P) are the polar coordinates of the projection of the observation point onto the (x,y)-plane, and $t_P \leftrightarrow t'_P$ stands for a set of terms like those already appearing on the right-hand side of (A 22) in which t_P and t'_P are everywhere interchanged.

The integrand of (A 22) can be written as $\partial^2 F/\partial\varphi\,\partial R_\perp$ where the primitive F is given by

$$\begin{aligned} F(R_\perp, \varphi) = \tfrac{1}{2}c^2 t_P^2 \{&[\varphi - \varphi_P - \arcsin(a\chi)]\,[\chi^{-2}(\operatorname{arccosh}\chi - \operatorname{arctanh} M^{-1}) \\ &-(1-\chi^{-2})^{\frac{1}{2}}] - a\chi^{-1}(1-a^2\chi^2)^{\frac{1}{2}}(\operatorname{arccosh}\chi - \operatorname{arctanh} M^{-1}) \\ &+\tfrac{1}{2}(a^2+1)\arcsin[|1-a^2|^{-1}(a^2+1-2a^2\chi^2)] \\ &+a \arcsin[|1-a^2|^{-1}(a^2+1-2\chi^{-2})]\}, \end{aligned} \tag{A 23}$$

with
$$a \equiv r_P \sin(\varphi - \varphi_P)/(ct_P). \tag{A 24}$$

By evaluating this primitive at the integration limits that appear in (A 22), we obtain

$$\begin{aligned} \int_N G_1\,\mathrm{d}x\,\mathrm{d}y\,\mathrm{d}\hat{z} = \tfrac{1}{2}c^2 t_P^2 \Bigg\{ &[\varphi_> - \varphi_P - \arcsin(\gamma a'_>)] \\ &\times\left[\left(\frac{t'_P}{\gamma t_P}\right)^2 \left(\operatorname{arccosh}\frac{\gamma t_P}{t'_P} - \operatorname{arctanh} M^{-1}\right) - \gamma^2 t_P^2 - t_P'^2)^{\frac{1}{2}}/(\gamma t_P)\right] \\ &- a_>^2(\gamma^{-2}a_>'^{-2} - 1)^{\frac{1}{2}}\left(\operatorname{arccosh}\frac{\gamma t_P}{t'_P} - \operatorname{arctanh} M^{-1}\right) \\ &+\tfrac{1}{2}(a_>^2+1)\arcsin[(a_>^2+1-2\gamma^2 a_>'^2)/(1-a_>^2)] \\ &+M^{-1}[\varphi_> - \varphi_P - \arcsin(\gamma a_>)] \\ &-\tfrac{1}{2}(a_>^2+1)\arcsin[(a_>^2+1-2\gamma^2 a_>^2)/(1-a_>^2)] \\ &-a_> \arcsin[(a_>^2 - 1 + 2M^{-2})/(1-(a_>^2)]\Bigg\} \\ &- t_P \leftrightarrow t'_P - \varphi_> \to \varphi_<, \end{aligned} \tag{A 25}$$

in which
$$\gamma \equiv (1-M^{-2})^{-\frac{1}{2}}, \qquad \text{A 26)}$$
$$a_{\gtrless} \equiv r_P \sin(\varphi_{\gtrless} - \varphi_P)/(ct_P), \tag{A 27a}$$
$$a'_{\gtrless} \equiv a_{\gtrless}\, t_P/t'_P, \tag{A 27b}$$

and $\varphi_> \to \varphi_<$, stands for a set of terms like those preceding it in which $\varphi_>$ is everywhere replaced by $\varphi_<$.

For arbitrary values of $a_{\gtrless}$ and $a'_{\gtrless}$, the right-hand side of (A 25) is an analytic function of the parameter T/t_P and can be expanded into a Taylor series to show that its value decays like T/t_P as $t_P \to \infty$. This corresponds, according to (A 26), to a sound field that decays spherically as $t_P \to \infty$. However, if we set the observation point in the neighbourhood of the truncated Mach cones which issue from the source distribution, and adopt the expression given in (A 18) for $\varphi_>$, then the contribution from $\varphi_>$ towards the value of (A 25) ceases to be analytic in T/t_P and turns out to possess a series expansion only in powers of $(T/t_P)^{\frac{1}{2}}$. The expression adopted for $\varphi_>$ in (A 18) renders the argument of $\arcsin(1-M^{-2})^{-\frac{1}{2}}a'_>$, which appears in (A 25), equal to unity and so represents the maximum value that can be assigned to $\varphi_>$ given the observation point.

From the expansion of the right-hand side of (A 25), as far as terms of the order of $(T/t_P)^3$, it now follows that, for $t_P \gg T$, the main contribution to the sound comes from the boundary $\varphi_>$ of N, and – to within the constant factor $\bar{s}$ – has the limiting value

$$\int_N G_1 \,\mathrm{d}x\,\mathrm{d}y\,\mathrm{d}\hat{z} = \frac{2\sqrt{2}}{15}(M-M^{-1})\,c^2T^2(T/t_P)^{\frac{1}{2}}+\ldots, \quad T/t_P \ll 1, \qquad \text{(A 28)}$$

at observation points that satisfy

$$(1-M^{-2})^{\frac{1}{2}} r_P^{-1} c t'_P \lesssim 1. \qquad \text{(A 29)}$$

(Note that source distrubution is assumed to be localized about $x = y = \hat{z} = 0$.) At such observation points, therefore, the amplitude of the radiation decays cylindrically, for ct_P is – according to (A 29) – proportional to r_P.

The part of the source which contributes towards the cylindrically decaying subpulse detected at P, i.e. neighbourhood N, has a $\hat{z}$-extent $\Delta\hat{z}$ which, as shown by (A 14) and (A 17), decreases like T/t_P as t_P increases. The observed width of this subpulse also decreases like T/t_P with t_P, because the collection of Mach cones issuing from the source points in N constitutes a conical shell whose $\hat{z}_P$-extent is the same as $\Delta\hat{z}$. The interval of retarded time Δt during which the subpulse in question is emitted, however, significantly differs from the short interval during which it is observed; the emission time Δt equals the entire lifetime of the source, T. If the retarded time t at which a source point (x, y, z_0) on the Mach cone makes its contribution towards the far field is t_0, then it follows from $R = c(t_P - t)$ and (A 5) that the corresponding value of t for the source point $(x, y, \hat{z}_0 + \Delta\hat{z}$ is $t_0 + \Delta t$ with $c\Delta t \approx M^{-\frac{1}{2}}(M^2-1)^{-\frac{1}{4}}(2R_P\Delta\hat{z})^{\frac{1}{2}}$ (Ffowcs Williams 1965). Had the extent $\Delta\hat{z}$ of the contributing source not been a decreasing function of t_P and so of R_P, the emission time interval Δt would have increased with R_P, like $R_P^{\frac{1}{2}}$. However, in the present case where Δt cannot exceed the lifespan of the source, T, it is $\Delta\hat{z}$ which decreases like R_P^{-1} and so renders Δt equal to T. The resulting subpulse has a width which correspondingly diminishes like R_P^{-1}. Thus, the long duration of the emission time interval – relative to that of the reception time interval – of the subpulse compensates for the slow decay of its amplitude to conserve its total energy.

The volume elements of the source within the lenticular part of the domain of dependence of the observation point P (figure 5) radiate cooperatively, over the entire lifetime of the source, to produce a coherent cylindrically decaying subpulse at P. The corresponding source elements for a neighbouring observation point likewise radiate in phase and produce a coherent subpulse, but a subpulse whose phase differs from that of the signal detected at P by a position-dependent retardation factor. Because there is one such subpulse associated with each observation point whose inverted Mach cone intersects the source distribution, the over-all waveform thus consists of an incoherent superposition of a (continuous) collection of coherent subpulses.

There is a cylindrically decaying component to the present radiation because the symmetry $\partial/\partial t + u\partial/\partial z = 0$ of the source density $s(x, y, \hat{z})$ transfers onto the field strength ρ itself and so reduces the dimension of the wave equation that governs the radiation by one: under this symmetry, the wave equation, (1), assumes the form

$$\frac{\partial^2\rho}{\partial x^2}+\frac{\partial^2\rho}{\partial y^2}-\left(\frac{u^2}{c^2}-1\right)\frac{\partial^2\rho}{\partial\hat{z}^2} = -4\pi s(x, y, \hat{z}). \qquad \text{(A 30)}$$

For $u > c$, therefore, the variable $\hat{z}/u$ plays the role of a time-like coordinate, and this reduced equation describes waves that propagate with the speed $(1-c^2/u^2)^{-\frac{1}{2}}c$ in the (x,y)-space. The wave fronts whose intersections with the (x,y)-plane travel with the supersonic speed $(1-c^2/u^2)^{-\frac{1}{2}}c$ are, in fact, those that interfere constructively to form the Mach cone. The Mach cone propagates with the speed c in the direction normal to itself, but by virtue of being inclined at the angle $\arccos(c/u)$ to a plane $z = \text{const.}$, it intersects such a plane along a circle that expands supersonically. Thus, the particular set of waves whose envelope constitutes the Mach cone, decay cylindrically, like two-dimensional waves.

Next, let us analyse this same problem in the frequency domain. By replacing the source density s in (A 3) with its Fourier representation

$$s(x,y,\hat{z}) = (2\pi)^{-1}\int_{-\infty}^{+\infty} \mathrm{d}k\,\tilde{s}(x,y,k)\exp(-\mathrm{i}k\hat{z}), \tag{A 31}$$

we can write the Fourier transform of the sound waveform p as

$$\tilde{p} = (2\pi)^{-1}\int \mathrm{d}x\,\mathrm{d}y\,\tilde{s}\int_0^T \mathrm{d}t\int_{-\infty}^{+\infty} \mathrm{d}\hat{z}\exp[-\mathrm{i}k(\hat{z}-\hat{z}_P)]\,\delta(t_P-t-R/c)/R, \tag{A 32}$$

where
$$\tilde{p} \equiv \int_{-\infty}^{+\infty} \mathrm{d}\hat{z}_P\exp(\mathrm{i}k\hat{z}_P)\,p, \tag{A 33}$$

and use has been made of (A 4). Evaluation of the $\hat{z}$-quadrature in (A 32) now yields

$$\tilde{p} = (2\pi)^{-1}\int \mathrm{d}x\,\mathrm{d}y\,\tilde{s}\int_0^T \mathrm{d}t\,\theta(\tau-R_\perp/c)\exp(-\mathrm{i}ku\tau) \times (c^2\tau^2-R_\perp^2)^{-\frac{1}{2}}\{\exp[\mathrm{i}k(c^2\tau^2-R_\perp^2)^{\frac{1}{2}}]+\exp[-\mathrm{i}k(c^2\tau^2-R_\perp^2)^{\frac{1}{2}}]\}, \tag{A 34}$$

in which $\tau \equiv t_P - t$.

Only the phase of the first term in the integrand of (A 34) has a stationary point, and this point occurs at

$$t_s = t_P - M(M^2-1)^{-\frac{1}{2}}R_\perp/c. \tag{A 35}$$

So, to obtain the leading contribution to the asymptotic value of $\tilde{p}$ for large k, we may approximate this phase by the following two terms in its Taylor expansion about $t = t_s$:

$$u\tau-(c^2\tau^2-R_\perp^2)^{\frac{1}{2}} = (M^2-1)^{\frac{1}{2}}R_\perp+\tfrac{1}{2}(M^2-1)^{\frac{3}{2}}R_\perp^{-1}c^2(t-t_s)^2+\dots, \tag{A 36}$$

and replace the amplitude of the integrand in (A 34) by its value at $t = t_s$. Provided that the Rayleigh parameter $k(cT)^2/R_\perp$ satisfies the constraint

$$k(cT)^2/R_\perp \gg (M^2-1)^{-\frac{3}{2}}, \tag{A 37}$$

we may in addition replace the range of integration in (A 34) by $(-\infty, +\infty)$. The resulting expression, then, is

$$\begin{aligned}\tilde{p} &\sim (2\pi)^{-1}(M^2-1)^{\frac{1}{2}}\int \mathrm{d}x\,\mathrm{d}y\,\tilde{s}R_\perp^{-1}\exp[-\mathrm{i}k(M^2-1)^{\frac{1}{2}}R_\perp]\int_{-\infty}^{+\infty}\mathrm{d}t \\ &\quad\times\exp[-\tfrac{1}{2}\mathrm{i}kc^2R_\perp^{-1}(M^2-1)^{\frac{3}{2}}(t-t_s)^2] \\ &\sim (2\pi)^{-\frac{1}{2}}\exp(-\tfrac{1}{4}\mathrm{i}\pi)\,c^{-1}(M^2-1)^{-\frac{1}{4}}k^{-\frac{1}{2}}\int \mathrm{d}x\,\mathrm{d}y\,\tilde{s}R_\perp^{-\frac{1}{2}}\exp[-\mathrm{i}k(M^2-1)^{\frac{1}{2}}R_\perp].\end{aligned} \tag{A 38}$$

This predicts that when the source occupies a localized region about $x = y = 0$, i.e.

$|x| \ll |x_P|$ and $|y| \ll |y_P|$ so that $R_\perp^2 \approx x_P^2 + y_P^2$, the sound decays cylindrically, like $(x_P^2+y_P^2)^{-\frac{1}{4}}$. In contrast to the outcome of the time-domain analysis, however, the validity of (A 38) is subject to the additional constraint (A 37) on the Rayleigh distance.

Amongst the source points with a given set of (x, y) coordinates, the one making the cylindrically decaying contribution towards the sound at $(x_P, y_P, \hat{z}_P)$ is that whose Lagrangian coordinate $\hat{z}$ has the value (A 9) and whose component of velocity in the radiation direction equals the wave speed at the time t_s given in (A 35): this value of t also follows from the time-domain analysis when the equation $t = t_P - R/c$, which is implied by the vanishing of the argument of the delta function in (A 4), is solved in conjunction with (A 9). According to the frequency-domain analysis, however, the strong contribution that is made at the time $t = t_s$ arises from all those source elements that share the coordinates (x, y), i.e. from a line source parallel to the $\hat{z}$-axis, and not from a neighbourhood of the single point on such a line source that lies on the inverted Mach cone (A 9). Just as in §4, therefore, the high-frequency approximation loses the information contained in the structure of the caustic (i.e. the Mach cone) along the spatial direction which is Fourier-analysed – in this case along $\hat{z}$ – and effectively treats the source as planar. The extra condition on the Rayleigh parameter stems from this limitation of the high-frequency approximation in situations where the sources and the fields depend on one of the space coordinates and the time in a single combination only (as in (A 2)), and is – for the reasons that are given at the end of §5 – spurious.

Appendix B. Gradient of the sound field

Our purpose in this appendix is to find the leading term in the asymptotic expansion, for $m \gg 1$ and $\hat{r}_P \gg 1$, of the following (regular) part of the gradient of the sound amplitude which follows from differentiating (15) under the integral sign:

$$\left(\frac{\partial \rho}{\partial \hat{r}_P}\right)_r = \mathrm{i} \sum_{m=-\infty}^{\infty} m\, \mathrm{e}^{\mathrm{i}m\hat{\varphi}_P} \int r\, \mathrm{d}r\, \mathrm{d}\varphi\, \mathrm{d}z \frac{s_m}{R} \frac{\partial g}{\partial \hat{r}_P} \mathrm{e}^{\mathrm{i}mg}, \tag{B 1}$$

in which

$$\partial g/\partial \hat{r}_P = (R\omega/c)^{-1} [\hat{r}_P - \hat{r}\cos(\varphi - \varphi_P)], \tag{B 2}$$

according to (5) and (9). We shall calculate this term by means of the method outlined in §§3 and 4.

Since, as we have already seen, the leading term in the asymptotic expansion in question arises from the filamentary part of the source which moves towards the observer at the wave speed with its normal parallel to the radiation direction, we may approximate $\partial g/\partial \hat{r}_P$ by its value at the cusp curve of the bifurcation surface. The angle φ appearing in (B 2) has the value (10) on the bifurcation surface ($\mathrm{d}g/\mathrm{d}\varphi = 0$), and the value $\varphi = \varphi_P + \arccos(\hat{r}_P^{-1}\hat{r}^{-1})$ on its cusp curve. For this latter value of φ and an observation point that is located in the far zone, (B 2) becomes

$$\partial g/\partial \hat{r}_P \approx \sin\theta_P. \tag{B 3}$$

Inserting (B 3) in (B 1) and comparing the resulting expression with (15), we find, therefore, that the asymptotic value of the mth Fourier component of $(\partial\rho/\partial\hat{r}_P)_r$ for $m \to \infty$ differs from the far-field value of the corresponding Fourier component of ρ given by (48) only in that it is multiplied by $\mathrm{i}m\sin\theta_P$.

REFERENCES

Abramowitz, M. & Stegun, I. A. 1970 *Handbook of Mathematical Functions*. Dover.

Ardavan, H. 1981 Is the light cylinder the site of emission in pulsars? *Nature* **287**, 44–45.

Ardavan, H. 1984 A speed-of-light barrier in classical electrodynamics. *Phys. Rev.* D **29**, 207–215.

ARDAVAN, H. 1989 The speed-of-light catastrophe. *Proc. R. Soc. Lond.* A **424**, 113–141.

ARDAVAN, H. 1991*a* The breakdown of the linearized theory and the role of quadrupole sources in transonic rotor acoustics. *J Fluid Mech.* **226**, 591–624.

ARDAVAN, H. 1991*b* The near-field singularity predicted by the spiral Green's function in acoustics and electrodynamics. *Proc. R. Soc. Lond. A* **433**, 451–459.

BLEISTEIN, N. & HANDELSMAN, R. A. 1986 *Asymptotic Expansions of Integrals.* Dover.

BRYAN, G. H. 1920 The acoustics of moving sources with applications to airscrews. *Rep. Mem. Aero. Res. Comm., Lond.* 648.

CHESTER, C., FRIEDMAN, B. & URSELL, F. 1957 An extension of the method of steepest descents. *Proc. Camb. Phil. Soc.* **54**, 599–611.

COSTA, A. A. DA & KAHN, F. D. 1985 Pulsar electrodynamics: the back reaction of the motion of charged particles. *Mon. Not. R. Astr. Soc.* **215**, 701–711.

COURANT, R. & HILBERT, D. 1962 *Methods of Mathematical Physics*, vol. 2. Interscience.

CRIGHTON, D. G. & PARRY, A. B. 1991 Asymptotic theory of propeller noise – Part II: Supersonic single-rotation propeller. *AIAA J.* **29**, 2031–2037.

DOWLING, A. P. & FFOWCS WILLIAMS, J. E. 1983 *Sound and Sources of Sound.* Ellis Horwood Ltd.

FARASSAT, F. 1981 Linear acoustic formulas for calculation of rotating blade noise. *AIAA J.* **19**, 1122–1130.

FARASSAT, F. & MYERS, M. K. 1989 An analysis of the quadrupole noise source of high speed rotating blades. Presented at *2nd IMACS Symp. on Computational Acoustics,* Princeton University.

FFOWCS WILLIAMS, J. E. 1965 On the development of Mach waves radiated by small disturbances. *J. Fluid Mech.* **22**, 49–55.

FFOWCS WILLIAMS, J. E. 1993*a* Computing the sources of sound. In *Computational Acoustics*, vol. I (ed. R. L. Lau, D. Lee & A. R. Robinson). Elsevier.

FFOWCS WILLIAMS, J. E. 1993*b* Supersonic sources make focused waves. In *Symposium on Aerodynamics and Aeroacoustics* (ed. K.-Y. Fung). World Scientific. (In press.)

FFOWCS WILLIAMS, J. E. & GUO, Y. P. 1988 Sound generated from the interruption of a steady flow by a supersonically moving aerofoil. *J Fluid Mech.* **195**, 113–135.

FFOWCS WILLIAMS, J. E. & HAWKINGS, D. L. 1969 Sound generation by turbulence and surfaces in arbitrary motion. *Phil. Trans. R. Soc. Lond. A* **264**, 321–342.

FRIEDLANDER, F. G. 1958 *Sound Pulses.* Cambridge University Press.

GUO, Y. P. 1990 Sound generation by a supersonic aerofoil cutting through a steady jet flow. *J. Fluid Mech.* **216**, 193–212.

HANSON, D. B. 1980 Helicoidal surface theory for harmonic noise of propellers in the far field. *AIAA J.* **18**, 1213–1220.

HANSON, D. B. 1983 Compressible helicoidal surface theory for propeller aerodynamics and noise. *AIAA J.* **21**, 881–889.

HANSON, D. B. & FINK, M. R. 1979 The importance of quadrupole sources in prediction of transonic tip speed propeller noise. *J. Sound Vib.* **62**, 19–38.

HAWKINGS, D. L. & LOWSON, M. V. 1974 Theory of open supersonic rotor noise. *J. Sound Vib.* **36**, 1–20.

HILTON, W. F. 1939 The photography of airscrew sound waves. *Proc. R. Soc. Lond.* A **169**, 174–190.

LIGHTHILL, M. J. 1993 Some aspects of the aeroacoustics of extreme-speed jets. In *Symposium on Aerodynamics and Aeroacoustics* (ed. K.-Y. Fung). World Scientific. (In press.)

LILLEY, G. M., WESTLEY, R., YATES, A. H. & BUSING, J. R. 1953 Some aspects of noise from supersonic aircraft. *J. R. Aero. Soc.* **57**, 396–414.

LUDWIG, D. 1966 Uniform asymptotic expansions at a caustic. *Commun. Pure Appl. Maths* **19**, 215–250.

MYERS, J., SHEN, H.-M., WU, T. T. & BRANDT, H. 1990 Fun with pulses. *Phys. World* **3**, (11), 39–42.

MYERS, M. K. & FARASSAT, F. 1987 Structure and propagation of supersonic singularities from helicoidal sources. *AIAA Paper* 87–2676.

PARRY, A. B. & CRIGHTON, D. G. 1989 Asymptotic theory of propeller noise – Part I: Subsonic single-rotation propeller. *AIAA J.* **27**, 1184–1190.

PEAKE, N. & CRIGHTON, D. G. 1991*a* Lighthill quadrupole radiation in supersonic propeller acoustics. *J. Fluid Mech.* **223**, 363–382.

PEAKE, N. & CRIGHTON, D. G. 1991*b* An asymptotic theory of near-field propeller acoustics. *J. Fluid Mech.* **232**, 285–301.

TAM, C. K. W. 1983 On linear acoustic solutions of high speed helicopter impulsive noise problems. *J. Sound Vib.* **89**, 119–134.

TAM, C. K. W., SALIKUDDIN, M. & HANSON, D. B. 1988 Acoustic interference of counter-rotation propellers. *J. Sound Vib.* **14**, 357–366.

WHITHAM, G. B. 1974 *Linear and Nonlinear Waves.* Wiley.

ZIOLKOWSKI, R. W. 1989 Localized transmission of electromagnetic energy. *Phys. Rev.* A **44**, 3960–3984.